



ARTICLE

IOTA-Based Authentication for IoT Devices in Satellite Networks

D. Bernal*, O. Ledesma, P. Lamo and J. Bermejo

Escuela Superior de Ingeniería y Tecnología, Universidad Internacional de La Rioja (UNIR), Av. de la Paz, 137, Logroño, 26006, La Rioja, Spain

*Corresponding Author: D. Bernal. Email: david.bernalaguera@unir.net

Received: 30 June 2025; Accepted: 17 October 2025

ABSTRACT: This work evaluates an architecture for decentralized authentication of Internet of Things (IoT) devices in Low Earth Orbit (LEO) satellite networks using IOTA Identity technology. To the best of our knowledge, it is the first proposal to integrate IOTA's Directed Acyclic Graph (DAG)-based identity framework into satellite IoT environments, enabling lightweight and distributed authentication under intermittent connectivity. The system leverages Decentralized Identifiers (DIDs) and Verifiable Credentials (VCs) over the Tangle, eliminating the need for mining and sequential blocks. An identity management workflow is implemented that supports the creation, validation, deactivation, and reactivation of IoT devices, and is experimentally validated on the Shimmer Testnet. Three metrics are defined and measured: resolution time, deactivation time, and reactivation time. To improve robustness, an algorithmic optimization is introduced that minimizes communication overhead and reduces latency during deactivation. The experimental results are compared with orbital simulations of satellite revisit times to assess operational feasibility. Unlike blockchain-based approaches, which typically suffer from high confirmation delays and scalability constraints, the proposed DAG architecture provides fast, cost-free operations suitable for resource-constrained IoT devices. The results show that authentication can be efficiently performed within satellite connectivity windows, positioning IOTA Identity as a viable solution for secure and scalable IoT authentication in LEO satellite networks.

KEYWORDS: Satellite IoT; decentralized authentication; directed acyclic graph; IOTA identity; verifiable credentials

1 Introduction

Global connectivity based on the Internet of Things (IoT) is experiencing rapid expansion, driven by the need to transmit data from devices located in remote or hard-to-reach regions. In this context, Low Earth Orbit (LEO) satellite constellations have been established as a key infrastructure for extending IoT communications coverage beyond the reach of traditional terrestrial networks [1,2]. Being at a lower altitude than geostationary satellites, LEO satellites reduce latency and increase link availability with devices, making them useful in applications such as fleet management, environmental monitoring, or autonomous vehicles [3,4]. To facilitate these communications, Low-Power Wide-Area Network (LPWAN) technologies are used, enabling the transmission of small volumes of data over long distances and in unlicensed frequency bands [5,6]. Among the LPWAN networks, Narrowband IoT (NB-IoT) stands out, having been included in Release 17 of the 3rd Generation Partnership Project (3GPP) as part of the 5G standard to enable IoT communications via satellite Non-Terrestrial Networks (NTN) [7,8]. This progressive expansion of IoT use cases, from terrestrial deployments to mobile and remote environments, also brings forward new security and authentication requirements. In this context, IoT devices were first deployed in industrial settings, where connectivity was generally stable and authentication relied on centralized mechanisms such as access



control lists and conventional network security protocols. With the subsequent expansion of IoT into unattended and mobile environments, including vehicles, ships, and drones, new challenges emerged due to intermittent connectivity and constrained device resources. These scenarios underscore the need for decentralized and resilient authentication schemes that can operate reliably under unstable communication conditions and within the limited computational and energy budgets characteristic of IoT devices [9]. However, the integration of IoT devices into satellite networks poses additional challenges in terms of security and access control [10]. Due to the open nature and wide coverage of satellite communications, these networks may be more vulnerable to interception, cyberattacks, and unauthorized access [11,12]. Furthermore, limited resource capacity and critical infrastructure underscore the importance of robust authentication and protection mechanisms [13] that ensure the availability, confidentiality, and integrity of services [14,15].

Protection strategies in these networks are articulated in various layers. In the top layer, traditional cryptographic techniques such as symmetric and public-key cryptography are employed [16,17]. However, their implementation in IoT devices is limited by computational and energy constraints [18]. In parallel, physical layer security (PLS) techniques have been proposed, which leverage channel properties such as noise or attenuation [19,20]. Additionally, the use of machine learning has been explored to detect anomalous patterns and mitigate attacks, such as DDoS. However, its practical application requires large volumes of data and efficient models for resource-limited environments [21,22]. Device authentication, as an entry point to satellite IoT networks, is therefore a critical security concern [23], which constitutes the first line of defense in satellite network architecture. In recent years, alternative schemes have been proposed, such as the use of zero-knowledge protocols based on modular codes [24] or the integration of blockchain and smart contracts to preserve privacy in cross-constellation collaboration [25,26]. However, centralized solutions and many blockchain architectures present scalability, flexibility, and latency limitations [9,27]. Faced with these limitations, new proposals based on Distributed Ledger Technology (DLT) are emerging, such as IOTA's Directed Acyclic Graph (DAG) [28] which allows the creation, storage and verification of Decentralized Identifiers (DIDs) and Verifiable Credentials (VCs) in an immutable manner, without the need for centralized validation entities [29,30]. This solution offers greater scalability, better privacy controls, and lower operating times than traditional alternatives or blockchain, making it especially suitable for dynamic and distributed environments, such as satellite IoT [31]. Despite the progress made with decentralized authentication mechanisms for IoT, the majority of proposals continue to be grounded in blockchain-based architectures. While these solutions offer transparency and immutability, they typically entail long confirmation times, significant energy consumption, and limited scalability when applied to resource-constrained environments, such as IoT and LEO satellite constellations. These limitations create a research gap for identity management frameworks that can operate efficiently within strict time windows, limited computational resources, and large-scale device populations. In particular, the suitability of DAG-based systems [32], notably IOTA Identity, for satellite-based IoT ecosystems has not yet been systematically analyzed. To address this gap, this work evaluates the performance of IOTA Identity for identity management in LEO satellite constellations, with an emphasis on credential resolution, deactivation, and reactivation. It offers a comparative perspective with blockchain-based authentication schemes, highlighting the potential of DAG-based approaches to overcome latency and scalability limitations [33]. In light of the above, this work aims to evaluate the technical feasibility of IOTA Identity as an authentication system for IoT devices in LEO satellite constellations. To this end, a distributed architecture implemented simulates the authentication process using DIDs. The resolution, deactivation, and reactivation times of digital identities are also empirically analyzed, comparing them with satellite revisit times. This research demonstrates the viability of IOTA Identity as a technology for authenticating IoT devices in LEO satellite environments.

For this purpose, the work is organized as follows: [Section 2](#) reviews the state-of-the-art in IoT identity management within the satellite environment. [Section 3](#) describes the developed technical architecture and the validation methodology used. [Section 4](#) presents the results obtained from the system and their comparison with orbital operating times. Finally, [Sections 5](#) and [6](#) present the discussion and conclusions.

2 State of the Art

The state of the art in authentication and identity management for IoT devices in satellite networks is multifaceted, encompassing traditional centralized approaches, blockchain-based solutions, and emerging DAG technologies. This section first reviews existing authentication methods, highlighting their limitations in resource-constrained and intermittent connectivity environments, which are typical of LEO satellites. It then examines the challenges associated with traditional blockchain architectures, such as high latency and scalability issues. Finally, it examines the benefits of DAG-based systems, such as IOTA, which provide lightweight, feeless operations suitable for decentralized IoT applications, laying the groundwork for the proposed integration in this work.

2.1 IoT, LEO Satellites and Protocols

The IoT has profoundly and transversally transformed all economic and social sectors, driving a new era of efficiency, automation, and data-driven decision-making. In agriculture, the IoT enables real-time monitoring of crops and soils, optimizing resource use and improving yields. In logistics, it facilitates the precise tracking of goods and fleets, increasing traceability and reducing operating costs. In precision agriculture, it optimizes production processes and decision-making, while in critical infrastructure, the IoT enables remote monitoring of parameters and device control. Thanks to the integration of smart sensors and advanced communication networks, the IoT is revolutionizing processes, enhancing productivity, and unlocking new opportunities for innovation in virtually all areas of society [\[34\]](#).

IoT devices connect to the Internet through wireless networks. This research examines the primary network protocols that utilize LPWAN technology. These protocols are designed to connect IoT devices that require low power consumption and long-distance transmission capacity [\[35\]](#). There are several types of LPWAN networks, each with specific characteristics and applications. Among the most notable technologies is LoRaWAN, which utilizes unlicensed spectrum and is employed in low-cost, long-range applications. Sigfox, an operator network that also operates in unlicensed bands, stands out for its simplicity and low power consumption. In contrast, NB-IoT, which uses licensed spectrum and leverages existing cellular infrastructure, offers higher penetration and reliability. They all differ in terms of spectrum type, speed, and ease of deployment. LoRaWAN and Sigfox stand out for their low cost and rapid implementation, while NB-IoT stands out for its robustness and reliability [\[36\]](#).

The integration of IoT technology with satellites in LEO orbit is revolutionizing global connectivity, enabling the connection and monitoring of critical infrastructure in remote and underserved regions [\[37\]](#). These satellites stand out for their small size and weight. They are made up of cubic-shaped modules called CubeSats, measuring 10 cm on each side and weighing approximately 1 kg each. Each cubesat can operate individually or in multi-unit configurations. They orbit the Earth at altitudes ranging from 500 to 1500 km. These satellites can mount communication antennas for different protocols, depending on the purpose of the satellite [\[38\]](#), offering low-latency coverage (20–50 ms) and higher transmission speeds than traditional geostationary satellites that orbit at higher altitudes [\[39\]](#). LEO satellites send a beep signal and activate the standby transmitters of IoT devices within their coverage area, allowing them to send data over the satellite link for as long as the satellite is available in their area, typically 5–10 min. There are two modes of connection

between IoT devices and LEO satellites: direct device-to-satellite connection (DtS-IoT) and indirect satellite connection (ItS-IoT), which involves installing an IoT gateway between the two devices [40].

Two physical effects directly affect the links between IoT devices and LEO satellites. On the one hand, the jitter effect is the variability in the arrival time of data packets at the satellite. This variability can be due to orbital dynamics factors or technological limitations and can especially impact time-sensitive applications, such as real-time device authentication and audio and video streaming. On the other hand, the Doppler effect, which causes a shift in the signal frequency due to the relative speed between the satellite and the ground device, necessitates constant synchronization adjustments and increases instability in packet delivery [41].

To increase the revisit frequency and provide more communication windows to each region on the Earth's surface, groups of satellites are launched into space, creating an orbiting constellation that operates in a coordinated manner, allowing for better coverage and redundancy across the planet's regions [42].

2.2 Existing Authentication Methods

IoT devices typically access the network through access control systems based on Public Key Infrastructure (PKI) and Network Access Control (NAC) protocols, such as 802.1x. These systems follow a centralized model that relies on key components, including certificate authorities (CAs), policy servers, and revocation repositories. In PKI, each device needs an X.509 certificate issued by a trusted root CA. NAC, in turn, uses credentials stored in central directories such as LDAP for authentication. These solutions are widely used in terrestrial environments, but have a limited geographic scope. However, they face challenges in geographically distributed IoT systems that rely on satellite connectivity. A major issue is the lack of synchronization with central servers. This leads to failures when renewing expired certificates, an inability to detect compromises via certificate revocation lists, and connection rejections due to timeouts, which typically occur within 2 to 5 s. Additionally, relying on a central server introduces a single point of failure. It also limits the scalability of the system when managing large numbers of connected devices [43,44]. Table 1 presents a comparison of the main access control and identity verification technologies, summarizing their capabilities in key aspects such as authentication, information management and sharing, interoperability between platforms, privacy protection, security mechanisms, and scalability potential. This comparison offers a comprehensive view of how each approach addresses the requirements of distributed systems, enabling the identification of their advantages and limitations in scenarios where trusted collaboration and data protection are essential.

Table 1: Comparison of identity and access control solutions

Feature	NAC 802.1x [45]	Centralized PKI	Blockchain	IOTA identity
Identity	Authorization through centralized certificate authorities.	Identities created and managed using centralized authorities [46].	Identities stored in a decentralized, immutable and distributed ledger [47].	Credentials stored and checked on a distributed ledger [48].
Identity verification	Authentication relies on centralized certificate authorities.	Depends on the integrity of the centralized authority and trust in their credentials [49].	Based on the validity of the DID and the associated public key [50].	Based on DIDs and verifiable credentials, not relying on centralized authorities [48].
Identity revocation	Certificate revocation depends on centralized lists, adding latency.	Revoking permissions relies on centralized databases. Slow and error-prone [51].	Deleting the DID revokes the identity, and the data cannot be altered [50].	Is decentralized, allowing users to revoke credentials without central authorities [48].

(Continued)

Table 1 (continued)

Feature	NAC 802.1x [45]	Centralized PKI	Blockchain	IOTA identity
Information shared	Limits sharing to specific attributes despite offering granular access control.	Allows minimal information sharing, often exposing sensitive data [52].	Allows sharing of specific attributes through the DID [53].	Allows granular control over the information shared. High flexibility [54].
Interoperability	Limited interoperability due to reliance on specific trust infrastructures.	High interoperability enables data sharing across various platforms and devices [52].	High interoperability due to their agnostic and decentralized design [55].	Widespread use in IoT enhances interoperability among various IoT devices and systems [56].
Privacy	Limited by the centralized storage of personal data.	Limited due to personal data being stored in centralized databases. Potential data leaks [57].	Depends on the design of the blockchain. Possibility of data leaks [58].	Data stored in a decentralized network. High confidentiality and user control [48].
Scalability	Limited by the capacity of centralized systems to handle users.	High. It can handle a large number of users [59].	High. It can handle many users, maintaining performance [60].	High. It can handle many users without performance degradation [61].
Security	Depends on robust encryption and a secure network infrastructure.	Can be compromised by attacks on centralized authorities [62].	High. Based on a decentralized network and cryptographic techniques [60].	Decentralization and strong cryptography enhance security and resilience against cyberattacks [48].

2.3 Extended Comparison of Identity Management and Authentication Solutions in IoT-Satellite Environments

The increasing integration of IoT devices in satellite environments poses significant challenges to identity management and access control, primarily due to the intrinsic resource limitations and intermittent connectivity in LEO satellite networks. Several technologies have been proposed and studied to address these challenges, each with particular strengths and limitations in terms of identity, privacy, scalability, security, and applicability to satellite access. Traditional network NAC-based systems employ a centralized access management model, offering moderate levels of privacy that aim to limit data exposure. They are not designed to support direct access in satellite environments due to the lack of methods adapted to latency and signal intermittency. PKI-based on digital signatures offers identity-centric authentication and access control mechanisms. However, they present privacy vulnerabilities and are prone to bottlenecks that hinder their scalability in massive networks. They also demonstrate a lack of robust techniques for distributed satellite environments [63]. The combination of PKIs with blockchain technologies introduces digital certificates and the management of DIDs, which improve interoperability and decentralization. However, privacy can be compromised by attacks targeting certification authorities, and scalability remains moderate due to the blockchain structure's dependence and associated costs [64,65]. On the other hand, blockchain-only approaches apply lightweight identification protocols and strong cryptography, facilitating the implementation of Self-Sovereign Identities (SSIs). These schemes offer proprietary control over private information, but demonstrate scalability limitations and a general lack of support for direct satellite access [66,67]. In contrast, DAG-based solutions such as IOTA Identity propose decentralized identity management using DIDs and VCs that incorporate advanced encryption, data sharing minimization, and SSI principles. IOTA's Tangle-based architecture offers high scalability due to its fee-free design and parallelizable validation, as well as robust security against spoofing attacks, unauthorized access, and other threats. However, these implementations did not initially consider satellite access. In this research, IOTA's DAG approach is extended by integrating allowlist-based NAC mechanisms tailored to the specific context of satellite IoT networks. This

solution provides a highly private, scalable, and secure identity and authentication model that incorporates end-to-end encryption and the immutability of the Tangle, ensuring resistance to impersonation, replay attacks, and unauthorized access. Furthermore, its viability for effective access and authentication in satellite environments with intermittent connectivity and resource constraints is demonstrated in [48] and this work. Table 2 summarizes the features of each type of solution.

Table 2: Comparison of authentication and identity technologies for satellite IoT access

Technology	Access control	Privacy	Scalability	Security	Satellite access
NAC [68]	Centralized 802.1x	Medium	Medium	Medium	No
PKI [63]	Cryptography, identity	Low	Low	Low	Yes
PKI, blockchain [64]	DID, certificates	Medium	Medium	High	No
PKI, blockchain [65]	SSI	Medium	Low	High	No
Blockchain [66]	Identification protocol	High	Low	High	No
Blockchain, NAC [67]	DID	High	Medium	High	No
DAG IOTA [48]	DID, VC	High	High	High	No
DAG IOTA (This work)	DID, VC, NAC	High	High	High	Yes

The system's strength stems primarily from the use of DIDs and VCs, both of which are anchored in the immutable, distributed ledger of IOTA. DIDs enable a strong cryptographic link between the digital identity and the unique key pair generated locally by system actors, i.e., IoT devices and satellite operators, thereby effectively eliminating the possibility of impersonation. Verifiable credentials, cryptographically signed using JSON Web Tokens (JWTs) by trusted issuing authorities, ensure the legitimacy and integrity of the attributes associated with each device, facilitating trusted authentication without exposing sensitive information [69]. The verification process incorporates critical mechanisms, such as the inclusion of nonces that prevent replay attacks and expiration fields that limit the validity of credentials, thus strengthening protection against malicious reuse. Cryptographic verification of signatures guarantees non-repudiation and maintains the unalterable integrity of the authentication and proof-providing process. Security guarantees are based on essential premises, including the maintenance of the Tangle's integrity and immutability, which ensures that identity states and revocation processes cannot be fraudulently altered. Furthermore, the cryptographic strength of the signature schemes employed protects against forgery and collisions. At the same time, the rigorous preservation of private keys under the exclusive control of legitimate actors prevents unauthorized access. The dynamic mechanism for deactivating and reactivating DIDs through IOTA ledger updates offers granular and flexible control over the identity lifecycle, preserving historical traceability. Although this research does not include formal demonstrations under standardized security models or experimental penetration tests, it clearly delineates the operational scenarios and adverse conditions under which the system maintains its robustness and correctness. The importance of future extensions that integrate formal validations and empirical evaluations using simulated attack scenarios to quantify the system's resilience to conflict situations in real-world environments is recognized.

2.4 Limitations of Traditional Blockchain

To address these limitations, DLT-based approaches have been proposed. These systems are distributed, allowing authentication to be decentralized. They rely on nodes connected via the Internet, each storing a copy of the network structure and all recorded transactions [70]. Some of these solutions are based on DLT-Blockchain. In this research, we analyzed uPort and Ceramic. Both are built on Ethereum and utilize

smart contracts to manage digital identities according to W3C standards [71]. They offer interoperability and benefit from a widely adopted network. However, blockchain-based architectures have critical limitations. The immutability of each block, the 15-s delay to confirm blocks, and the high transaction fees paid by users make blockchain unsuitable for IoT authentication. IoT devices require dynamic methods that can quickly allow or deny access to the network, depending on real-time conditions.

2.5 Advantages of DAG/IOTA

An alternative to blockchain is the Tangle. It is a DAG that allows fast and feeless transactions with high scalability. This technology removes the barriers that limit the adoption of distributed systems in IoT. With the Tangle, machines can exchange data and value seamlessly through Machine-to-Machine (M2M) communication. Its architecture avoids centralized validation. Instead, each user or device actively participates in the network consensus. The Tangle is the technological core of IOTA and differs from traditional blockchains in that it does not use blocks; alternatively, it relies on a peer-to-peer network to validate transactions. Rather, each new transaction must confirm two previous transactions, creating a distributed validation structure that eliminates the bottlenecks present in traditional systems. This model offers advantages in terms of scalability, as there is no fixed limit on the number of transactions that can be processed simultaneously. As network activity increases, the Tangle strengthens, improving both validation speed and participant decentralization. The consensus process in IOTA is based on a completely participatory mechanism, where each user contributes to the system's security and integrity. To ensure the integrity of transactions, the Tangle follows three phases. Before recording a new transaction, a node must verify two previous ones, ensuring the continuity of the validation process. In addition, a small amount of computational work is performed to prevent spam on the network. When a new transaction is issued, others must directly or indirectly select it as a reference for validation. This model eliminates the need for miners, allowing the system to grow without relying on a central authority. Finally, IOTA employs the Random Walk Monte Carlo algorithm, which selects two random transactions to be validated with each new issuance. Over time, a transaction gains trust as other transactions reference it [72]. IOTA incorporates a DLT-based digital identity framework called IOTA Identity. A key element of this framework is the use of DIDs, which are unique identifiers generated and controlled by the user without the need for a central authority. A DID document represents a unique digital identity for a device or entity on the IOTA network, providing a trusted framework for secure interactions and transactions in the decentralized ecosystem. The integration of IOTA Identity with DIDs represents an evolution in how identity is managed in digital environments, fostering greater security, autonomy, and transparency in credential management. Ensuring that credentials are secure, persistent, and verifiable without the need for centralized databases. The DID is a structured JSON file that includes data about cryptographic keys, communication methods, or permission policies. This file is stored in the Tangle and accessed through its alias, a string of 30 to 50 characters that begins with "did:iota:." IOTA Identity enables the autonomous creation, management, and sharing of credentials, eliminating the need for intermediaries [73]. This approach is based on the concept of Self-Sovereign Identity (SSI), where each individual, organization, or device maintains absolute control over their information, deciding what data to share and with whom. This identity system is structured into three fundamental roles: holders, who are the owners of digital identities; issuers, trusted entities that issue verifiable certificates, such as identity documents; and verifiers, third parties that validate the authenticity of data provided by Holders [32]. It also enables agile and flexible credential management, making it useful in networks where devices may require frequent changes to their access permissions, as occurs in dynamic, distributed scenarios where external events condition access. Furthermore, it provides granularity in the control of authentication data, which represents an improvement over conventional models, where certificates typically include fixed and

complete subject information [74]. A comparative analysis with other decentralized identity frameworks further clarifies the relevance of IOTA Identity in the context of satellite-based IoT. uPort [75], as one of the earliest implementations of DIDs on Ethereum, inherits the transaction costs, confirmation delays, and scalability limitations of blockchain infrastructures, which are incompatible with the latency and cost constraints of LEO satellite communications. Ceramic [76] introduces greater flexibility for data streams and off-chain document management. However, its reliance on periodic anchoring to linear blockchains still imposes finality delays and additional complexity that hinder real-time or near-real-time authentication [77]. In contrast, IOTA Identity leverages the parallelizable validation of the Tangle to provide cost-free operations with low confirmation times, aligning with the stringent constraints of intermittent connectivity windows and resource-constrained IoT devices in satellite networks. This distinction highlights the suitability of DAG-based identity management for ensuring continuous, lightweight, and efficient authentication in scenarios where blockchain-based solutions face structural limitations.

The novelty of this research lies in the application of DLT technology to secure the process of controlling access to the satellite environment for IoT devices dispersed across the Earth's surface. Ensuring that only authorized devices can access the system and offering a streamlined process for deactivating or reactivating IoT devices' permissions to access the satellite system.

2.6 Security Frameworks and Modern Methodologies

Recent advances in IoT-satellite integration have increasingly adopted security paradigms that move beyond traditional perimeter-based defenses. Among these, Zero Trust Architecture (ZTA) has emerged as a dominant framework, premised on the principle of “never trust, always verify” [78,79]. In a ZTA context, every entity, whether a device, service, or user, must undergo continuous authentication and authorization based on dynamic policy evaluation, regardless of its network location. This contrasts with earlier models that assumed inherent trust for devices within a predefined network boundary, an assumption that is particularly unsuitable in satellite-IoT ecosystems with intermittent connectivity and heterogeneous device profiles. Related studies have explored the integration of ZTA with distributed ledger technologies to strengthen device identity assurance and reduce reliance on centralized trust anchors [80]. In these approaches, verifiable credentials and decentralized identifiers are used to enforce policy decisions at each transaction or session establishment, leveraging immutable logs for auditability and compliance. Other works combine ZTA principles with secure enclaves and hardware roots of trust, enabling cryptographic attestation of device integrity prior to granting network access [81]. Despite these advances, implementing zero trust in resource-constrained IoT devices that communicate through LEO satellites remains challenging due to the computational cost of continuous verification, the need for efficient policy decision points that can operate under high-latency conditions, and the complexity of revocation in decentralized contexts. Our proposed IOTA-based authentication framework aligns with ZTA principles by enforcing verification at each authentication event, eliminating implicit trust, and enabling ledger-anchored revocation checks. However, unlike conventional ZTA deployments, the reliance on the Tangle as a DAG-based DLT provides scalability advantages. It removes the dependency on centralized policy databases, thereby reducing single points of failure and potential bottlenecks in satellite communication links. On the security front, the system employs a layered defense-in-depth approach tailored for LPWAN satellite communications over LoRaWAN and NB-IoT. Each IoT node is provisioned with a unique cryptographic identity, stored within a secure hardware element to resist tampering. Data payloads are encrypted end-to-end using AES-128 in the case of LoRaWAN [82], while NB-IoT leverages 3GPP-standardized LTE-grade security mechanisms, including mutual authentication and integrity protection [83]. To prevent tampering, message authentication codes (MACs) are appended, and replay attacks are mitigated through sequence counters or timestamping. The

satellite and ground/cloud segments of the architecture establish secure tunnels based on TLS or DTLS, ensuring confidentiality and integrity during backhaul transmission. Furthermore, network servers and core platforms enforce fine-grained access control policies to prevent unauthorized queries or command injection, thereby complementing the ZTA principles applied at the device and ledger levels.

3 Methodology

In light of the properties of the various authentication technologies analyzed, it is necessary to consider the intrinsic characteristics of satellite connections in LEO, specifically the intermittent communication windows, which last between 2 and 5 min per pass, and the payload limitations inherent in LPWAN protocols. This maximum can range between 51 and 222 bytes, depending on the transmission mode. Adding limitations to the authentication process because the size of the messages sent by DLT technologies during authentication exceeds the frame size limit. This limitation means that the authentication process cannot be initiated directly on the IoT device and must be managed from the ground station, where broadband connectivity enables the generation of DID Documents and VCs outside the satellite infrastructure, thereby minimizing the computational load in orbit and overcoming bandwidth and payload limitations. Although satellite-to-ground downlinks offer greater bandwidth (1–10 Mbps), resource optimization in the space segment prioritizes storing only the necessary keys as a device allowlist for access control. Intensive operations, including identity creation, updating, and revocation, are offloaded to the ground infrastructure, where critical tasks such as these are performed efficiently due to the absence of bandwidth or processing limitations. This strategy overcomes the restrictions imposed by the small frame size of LPWAN protocols.

During the registration or onboarding phase of each IoT device, a DID document compliant with the W3C standard is generated and associated with a unique device identifier, which can be a MAC address, a serial number, or any other data that uniquely identifies it. The DID document is registered in the IOTA Tangle, thus creating an immutable and globally accessible record. When the IoT device needs to authenticate itself to the satellite, it transmits its DID identifier in an optimized frame that takes up minimal space within the payload allowed by LPWAN [35]. The satellite, for its part, maintains a local access control allowlist, storing authorized DID identifiers. This list is updated periodically, leveraging communication windows with the ground station by downloading cryptographic proofs (Merkle Proofs) from the Tangle, which enables verification that the DIDs associated with the IoT devices have not been revoked. In this way, authentication and access control are performed efficiently and securely without overloading satellite communications and ensuring that only authorized devices can interact with the system, even in scenarios of intermittent connectivity and extremely limited resources. Recent literature has not evaluated the applicability of these technologies in emerging satellite environments. Therefore, this research proposes to evaluate the technical feasibility of IOTA Identity as a distributed authentication mechanism for IoT devices in a LEO-based satellite communications architecture. To this end, a distributed infrastructure has been developed that replicates a realistic satellite environment and implements a complete digital identity management workflow using DIDs and VCs stored on the IOTA Tangle network.

3.1 Distributed Architecture for IoT Identity Management

The used physical architecture comprises five main entities: IoT devices, LEO satellites, ground stations, the Tangle network, and an IoT platform that centralizes validation and monitoring operations (Fig. 1). The IoT devices, located in remote areas, capture physical data and transmit messages over LPWAN links to LEO satellites that periodically fly over the coverage area.

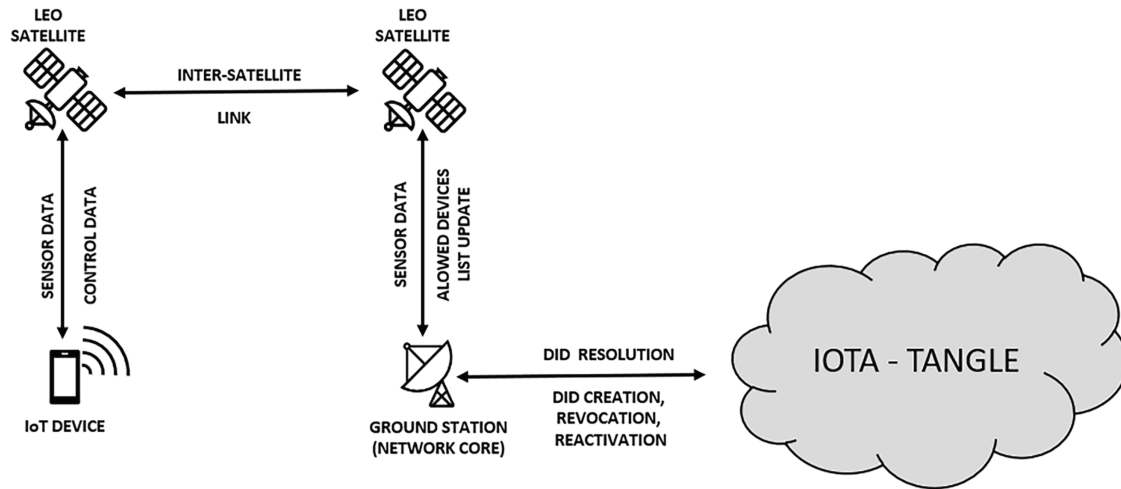


Figure 1: Conceptual IoT-satellite architecture

Satellites serve as mobile access nodes, managing device authorization to access their infrastructure before accepting transmissions and temporarily storing the data until a link is established with a ground station. Subsequently, ground stations take over by querying the Tangle to resolve DIDs and verify device legitimacy, then update the device allowlist. The Tangle, functioning as a distributed, immutable database, enables the asynchronous storage and retrieval of these identities, supporting the ground-based validation process. Ground stations transfer the updated list to the satellite as soon as it enters their coverage area.

3.2 Decentralised Authentication Process

The lifecycle of DIDs in the proposed architecture encompasses the phases of creation, credential issuance, presentation, validation, deactivation, and reactivation. While each of these steps is detailed algorithmically in the manuscript, their integration is now complemented with a concise summary presented in Table 3, which organizes the core functions, actors involved, and security mechanisms supporting each stage of the lifecycle.

Table 3: Summary of security assumptions for the DID lifecycle

Phase	Description	Security assumptions
Creation	A DID is generated by the IoT device and registered in the Tangle through a ground station.	Trust in ground stations for reliable DID anchoring.
Issuance	Verifiable credentials are issued and cryptographically signed by the authority.	Integrity of the issuer's private keys.
Presentation	Devices present credentials to request authentication with the satellite gateway.	Secure communication channel for credential exchange.
Validation	Verifiers check the DID state and credential signatures against the Tangle.	Availability and consistency of the distributed ledger.

(Continued)

Table 3 (continued)

Phase	Description	Security assumptions
Deactivation	A DID is marked as inactive in the event of compromise or lifecycle termination.	Proper propagation of revocation status across the network.
Reactivation	A previously deactivated DID is reinstated after verification of authenticity.	Robust temporal synchronization to prevent replay or race conditions.

The methodological design relies on a set of explicit security assumptions. Ground stations are considered trusted entities, ensuring the correct orchestration of initial communication and propagation of updates. Time synchronization across the network is assumed to be robust enough to preserve consistency in transaction ordering and credential validation. Within these assumptions, the cryptographic mechanisms supporting DID management—namely creation, validation, revocation, and reactivation can be reliably deployed to prevent impersonation or tampering. IOTA Identity provides a framework for developing the decentralized identity management process for IoT devices in a satellite environment. The steps required to manage everything from DID creation to revocation are as follows:

3.2.1 DID Creation

Each IoT device and each satellite operator has a unique DID generated from a cryptographic key pair that complies with W3C specifications. The identifier is registered in the Tangle using a DID document that links an Alias ID to the device's attributes (e.g., MAC address, serial number). This initial creation is performed outside the satellite channel to avoid interfering with the connectivity window. The generated DID addresses are included in the document as unique and traceable identifiers. Algorithm 1 shows the sequential steps for generating and registering the DIDs of both the IoT device and the satellite operator, establishing the basis for the trust model between the issuer and the holder.

Algorithm 1: Creation of decentralized identities

- 1: **Step 1: Creation of decentralized identities for the issuer and the holder.**
 - 2: **1. Initialize client to connect to the Tangle:**
 - 3: a. Create a client object with configuration parameters.
 - 4: **2. Initialize identity client:**
 - 5: a. Create an identity client object using the previously created client.
 - 6: **3. Create a new wallet and identity for the satellite operator:**
 - 7: a. Generate a mnemonic phrase for the satellite operator.
 - 8: b. Create storage for the satellite operator's identity.
 - 9: **4. Create a new wallet and identity for the IoT device:**
 - 10: a. Generate a mnemonic phrase for the IoT device.
 - 11: b. Create storage for the IoT device's identity.
 - 12: **5. Create DID for the satellite operator:**
 - 13: a. Use the client, secret manager, and storage to create the satellite operator's DID.
 - 14: b. Obtain the document and the fragment of the created DID.
-

(Continued)

Algorithm 1 (continued)

15: **6. Create DID for the IoT device:**

16: a. Use the client, secret manager, and storage to create the IoT device's DID.

17: b. Obtain the document and the fragment of the created DID.

Below is the result of executing the code to create a DID for the IoT device and the satellite operator. (see Fig. 2). The DIDs have been stored in the IOTA Test Tangle (Testnet) with the following addresses:

```

Wallet address Bech32: rms1qz625s0cydxqs435et59c56ktcmtkra32mmy62t9xktltqjnjxqpz7ktscf
Sat Company DID {
  id: 'did:iota:rms:0x9d860dba6e6b257b8ac13b0cf38d1f18bfc62a014cf5084e51567b746a65d2bd',
  assertionMethod: [
    {
      id: 'did:iota:rms:0x9d860dba6e6b257b8ac13b0cf38d1f18bfc62a014cf5084e51567b746a65d2bd#jwk',
      controller: 'did:iota:rms:0x9d860dba6e6b257b8ac13b0cf38d1f18bfc62a014cf5084e51567b746a65d2bd',
      type: 'JsonWebKey',
      publicKeyJwk: [Object]
    }
  ]
}
Wallet address Bech32: rms1qrv8pnelnerp0y7a468vlj8zg8mnsfk0yga4tmxa874wphjqxs40uxg34xq
IoT Device DID {
  id: 'did:iota:rms:0x3117cad033f5500efe75d70256e14742a258e2cdb90fc2c3ec0e3752f2d4bf67',
  assertionMethod: [
    {
      id: 'did:iota:rms:0x3117cad033f5500efe75d70256e14742a258e2cdb90fc2c3ec0e3752f2d4bf67#jwk',
      controller: 'did:iota:rms:0x3117cad033f5500efe75d70256e14742a258e2cdb90fc2c3ec0e3752f2d4bf67',
      type: 'JsonWebKey',
      publicKeyJwk: [Object]
    }
  ]
}

```

Figure 2: Result of the creation of DIDs for issuer and holder

DID address of the IoT device:

◦ did:iota:rms:0x3117cad033f5500efe75d70256e14742a258e2cdb90fc2c3ec0e3752f2d4bf67.

Satellite operator DID address

◦ did:iota:rms:0x9d860dba6e6b257b8ac13b0cf38d1f18bfc62a014cf5084e51567b746a65d2bd.

Figs. 3 and 4 show the DID information stored in the IOTA Tangle for the issuer and holder.

3.2.2 Issuance of the Verifiable Credential


Once the device's DID is created, the satellite operator, in its role as a trusted issuing authority, generates a VC for the device. This credential contains the device's identifying attributes, is serialized in JWT format, and is cryptographically signed using the issuer's private key. This signature ensures the integrity of the credential and authenticates it as issued by a legitimate authority. Algorithm 2 details the process of defining the credential content, generating the JWT, and initially validating it. Verifiable credentials are not stored in the Tangle but rather in secure systems outside the network to preserve their confidentiality and prevent unauthorized access.

Alias

General

Alias Address
zms1pqc38jksx064qzh7whtsy4hpgap2yk8zekuslskxas8zw5hj6j1kw0uwlsm

Alias Id
0x3117cad033f5500efe75d70256e14742a258e2cdb90fc2c3ec0e3752f2d4bf67


Available Balance
0

Storage Deposit
0.08 SMR

State
Foundries
DID
Transactions
Native Tokens
NFTs
Associated Outputs

DID
did:iota:rms:0x3117cad033f5500efe75d70256e14742a258e2cdb90fc2c3ec0e3752f2d4bf67

Governor
zms1qrv8pnelnerp0y7a468vlj8zg8mnsfk0yga4tmxa874wphjqxs40uxg34xq

State Controller
zms1qrv8pnelnerp0y7a468vlj8zg8mnsfk0yga4tmxa874wphjqxs40uxg34xq

Linked Domains
no linked domains

DID Document

```

{
  "id": "did:iota:rms:0x3117cad033f5500efe75d70256e14742a258e2cdb90fc2c3ec0e3752f2d4bf67",
  "assertionMethod": [
    {
      "id": "did:iota:rms:0x3117cad033f5500efe75d70256e14742a258e2cdb90fc2c3ec0e3752f2d4bf670jwk",
      "controller": "did:iota:rms:0x3117cad033f5500efe75d70256e14742a258e2cdb90fc2c3ec0e3752f2d4bf67",
      "type": "JsonWebKey",
      "publicKeyJwk": {
        "kty": "OKP",
        "alg": "EdDSA",
        "crv": "Ed25519",
        "x": "6P-VJkoV9VCy8XZnMFVBjx7Qk3FZ37LBQ4ASZnJPkzM"
      }
    }
  ]
}

```

Metadata

```

{
  "created": "2024-01-24T22:03:12Z",
  "updated": "2024-01-24T22:03:12Z",
  "governorAddress": "zms1qrv8pnelnerp0y7a468vlj8zg8mnsfk0yga4tmxa874wphjqxs40uxg34xq",
  "stateControllerAddress": "zms1qrv8pnelnerp0y7a468vlj8zg8mnsfk0yga4tmxa874wphjqxs40uxg34xq"
}

```


Figure 3: IoT device DID stored in the tangle

Alias

General

Alias Address
rms1pzwcvr6de4j27u2cyaseuudruvtl332q9x02zzw29t8kar2vht64ga6j6

Alias Id
0x9d860dba6e6b257b8ac13b0cf38d1f18bfc62a014cf5084e51567b746a65d2bd



Available Balance

0

Storage Deposit

0.08 SMR

State
Foundries
DID
Transactions
Native Tokens
NFTs
Associated Outputs

DID
did:iota:rms:0x9d860dba6e6b257b8ac13b0cf38d1f18bfc62a014cf5084e51567b746a65d2bd

Governor
rms1qz625s0cydxqs435et59c56ktcmkra32mmy62t9xktltqjnjqxz7ktsf

State Controller
rms1qz625s0cydxqs435et59c56ktcmkra32mmy62t9xktltqjnjqxz7ktsf

Linked Domains
no linked domains

DID Document

```
{
  "id": "did:iota:rms:0x9d860dba6e6b257b8ac13b0cf38d1f18bfc62a014cf5084e51567b746a65d2bd",
  "assertionMethod": [
    {
      "id": "did:iota:rms:0x9d860dba6e6b257b8ac13b0cf38d1f18bfc62a014cf5084e51567b746a65d2bd#jwk",
      "controller": "did:iota:rms:0x9d860dba6e6b257b8ac13b0cf38d1f18bfc62a014cf5084e51567b746a65d2bd",
      "type": "JsonWebKey",
      "publicKeyJwk": {
        "kty": "OKP",
        "alg": "EdDSA",
        "crv": "Ed25519",
        "x": "KWsxdJz9KWu-pzYfC11oXzWHZfntBzYRK_x86Fn5Q"
      }
    }
  ]
}
```

Metadata

```
{
  "created": "2024-01-24T22:02:33Z",
  "updated": "2024-01-24T22:02:33Z",
  "governorAddress": "rms1qz625s0cydxqs435et59c56ktcmkra32mmy62t9xktltqjnjqxz7ktsf",
  "stateControllerAddress": "rms1qz625s0cydxqs435et59c56ktcmkra32mmy62t9xktltqjnjqxz7ktsf"
}
```

Figure 4: Satellite operator DID stored in tangle

Algorithm 2: Generation and validation of verifiable credentials for IoT devices

```

1: Step 2: Define IoT Device Data
2:   a. Define device id
3:   b. Define device name
4:   c. Define device specific_information
5:   Step 3: Create Unsigned Verifiable Credential
6:     a. Set unique credential_id
7:     b. Set credential_type  $\leftarrow$  "IoTDeviceInfoCredential"
8:     c. Set issuer  $\leftarrow$  id of the satellite company
9:     d. Set credential_subject  $\leftarrow$  IoT Device Data (id, name, specific_information)
10:    Step 4: Sign the Verifiable Credential
11:      a. Use the satellite company's private key to sign the unsigned_credential
12:      b. Generate jwt_token  $\leftarrow$  JWT containing the signed_credential
13:    Step 5: Validate the Signed Credential
14:      a. Use a signature verifier to validate the jwt_token
15:      — Begin validation process —
16:        If jwt_token is valid and not expired:
17:          Credential valid: proceed to the next step
18:        Else:
19:          Report error: Credential invalid or expired
20:      — End validation process —

```

As a result of executing Algorithm 2, a verifiable credential is created for the IoT device (see Fig. 5).

```

credentialjwt validation {
  '@context': 'https://www.w3.org/2018/credentials/v1',
  id: 'https://example.edu/credentials/3732',
  type: [ 'VerifiableCredential', 'IoTDeviceInfoCredential' ],
  credentialSubject: {
    id: 'did:iota:rms:0x3117cad033f5500efe75d70256e14742a258e2cdb90fc2c3ec0e3752f2d4bf67',
    GPS: '41.40338, 2.17403',
    name: 'Humidity Sensor',
    sensorMAC: '00:1B:44:11:3A:B7',
    sensorType: 'LoRa IoT Sensor'
  },
  issuer: 'did:iota:rms:0x9d860dba6e6b257b8ac13b0cf38d1f18bfc62a014cf5084e51567b746a65d2bd',
  issuanceDate: '2024-01-24T22:03:30Z'
}

```

Figure 5: Result of creating verifiable credentials

3.2.3 Generation and Submission of Verifiable Presentation

Each time an IoT device requires authentication, it generates a verifiable presentation (VP) that encapsulates the previously issued VC, along with cryptographic proof of possession of its private key. This presentation includes a nonce (cryptographic challenge) and an expiration field to prevent replay attacks and ensure that the credentials are valid only within a specified time interval. Algorithm 3 describes the procedure for generating the presentation, signing it with the device's private key, and sending it to the verifier.

Algorithm 3: Creation and sending of a verifiable presentation

-
- ```

1: Step 6: Create Verifiable Presentation
2: 1. Create the Verifiable Presentation
3: a. Set the presentation holder (id of the IoT device).
4: b. Include the verifiable credential signed by the satellite operator.
5: 2. Sign the Presentation
6: a. Use the IoT device's key to sign the presentation.
7: b. Generate a JWT token containing the signed presentation.
8: c. Include a nonce to prevent replay attacks.
9: d. Set an expiration date for the presentation.
10: Step 7: Send the Verifiable Presentation
11: 1. Send Presentation
12: a. Send the signed presentation (as a JWT) to the verifier.

```
- 

As a result of executing Algorithm 3, a verifiable presentation is created that the IoT device can use to prove its identity (see Fig. 6).

```

Sending presentation (as JWT) to the verifier {
 '@content': 'https://www.w3.com/2028/credentials/V1',
 type: 'VerifiablePresentation',
 verifiableCredential: [
 'eyJX7p9Jq2M4a5D8k1L6t3W0fZcNyVbGrSeUoHxliM2g7Q1a9D4p5J8t6L0f3WzCnYvBrdd
 SeUoHxKiT8p4Jq9M2a5D7k1L6wOfZcNyVbGrSeUoHxlgL6m2G7q9A5d8P4j1TOF3WzCnY
 vBrSeUoHxliF3t8P4jQ9m2A7d5K1I6W0zCnYvBrSeUoHxliF3t8P4jQ9m2A5D7k1L6wOfZcNyVbGrSeUoHxe7
 IgL6m2G7q9A5d8P4j1TOF3WzCnYvBrSeUoHxliF3t8P4jQ9m2A7d5K1I6W0zCnYvBrSeU6T
 oHxliZcNyVbGrSeUoHxKi7nYvBrSeUoHxliZcNyVbGrSeUoHxKi7P9jQ2f4hyUJw2cxs9jeoL
 M4a5D8K1I6T3W0fZcNyVbGrSeUoHxliM2G7q1A9D4P5j8T6IOF3WzCnYvBrSeUoHxKiT81
 P4jQ9m2A5d7K1L6wOfZcNyVbGrSeUoHxlgL6m2G7Q9a5D8p4J1TOF3WzCnYvBg'
],
 holder:
 did:iota:rms:Ox3117cad033f5500efe75d70256e14742a258e2cdb90fc2c3ec0e3752f2d4bf67'
}

```

**Figure 6:** Result of creating verifiable presentation

### 3.2.4 Verification of the Presentation

The verifier, depending on the use case, could be an accredited verification entity or the satellite operator itself, and executes a complete validation process of the verifiable submission received:

- Validation of the JWT signature of the presentation.
- Verifying the nonce and expiration date.
- Resolving the issuer's DID in the Tangle to extract the original DID document.
- Validation of the verifiable credential signature and verification of its integrity.
- Confirmation that the credential subject matches the presentation holder.

This process is represented in Algorithm 4 and guarantees the authenticity of the device, the integrity of the authentication channel, and the traceability of the credential issuer. If successful, the device is temporarily registered as authorized to transmit data over the satellite channel.

---

**Algorithm 4:** Verification of a verifiable presentation

---

- 1: **Step 8: Verification of the Verifiable Presentation**
  - 2: **1. Reception and Initial Processing**
  - 3:     a. Receive the JWT presentation from the IoT device.
  - 4: **2. Presentation Validation**
  - 5:     a. Use a signature verifier to validate the JWT presentation.
  - 6:     b. Check that the presentation is valid and has not expired.
  - 7: **3. Holder Resolution**
  - 8:     a. Resolve the Decentralized Identifier (DID) of the presentation holder.
  - 9: **4. Credential Validation**
  - 10:    a. Extract the verifiable credentials from the presentation.
  - 11:    b. Resolve the issuers of the credentials.
  - 12:    c. Validate each credential using the resolved issuer information.
  - 13:    d. Ensure that the credentials are valid and satisfy the required relationship between subject and holder.
- 

**3.2.5 Dynamic Deactivation and Reactivation of the DID**

As shown in Algorithm 5, access revocation is implemented by updating the document associated with the DID's Alias ID and replacing it with an empty document. This approach enables the identity to be deactivated without deleting the root DID, allowing for subsequent reactivation by restoring the original document. This operation can be performed by the system administrator or the device owner, offering granular control over the identity lifecycle without compromising the system's traceability or historical integrity.

---

**Algorithm 5:** Deactivation and reactivation of a decentralized identifier

---

- 1: **Step 9: Deactivate DID**
  - 2: **1. Prepare Deactivation Request**
  - 3:     a. Identify the DID to be deactivated.
  - 4:     b. Retrieve the necessary private key or control delegation for deactivation.
  - 5:     c. Construct a DID deactivation operation or document update.
  - 6:     d. Include any required revocation information or updates on status.
  - 7: **2. Sign the Deactivation Request**
  - 8:     a. Use the authorized private key to sign the deactivation request.
  - 9: **3. Submit Deactivation to Tangle**
  - 10:    a. Publish the signed deactivation operation to the Tangle.
  - 11:    b. Ensure the transaction is confirmed according consensus mechanism.
  - 12: **4. Verify Deactivation**
  - 13:    a. Query the ledger for the status of the DID.
  - 14:    b. Confirm that the DID document now reflects the DEACTIVATED state.
  - 15: **Step 10: Reactivate DID**
  - 16: **1. Prepare Reactivation Request**
  - 17:    a. Identify the deactivated DID to be reactivated.
  - 18:    b. Retrieve the necessary private key or control delegation for reactivation.
  - 19:    c. Construct a DID reactivation operation or document update.
- 

(Continued)

**Algorithm 5 (continued)**

- 20: d. Ensure the reactivation is permissible according to any defined policies or time constraints.
- 21: **2. Sign the Reactivation Request**
- 22: a. Use the authorized private key to sign the reactivation request cryptographically.
- 23: **3. Submit Reactivation to the Tangle**
- 24: a. Publish the signed reactivation operation to the Tangle.
- 25: b. Ensure the transaction is confirmed according to the ledger's consensus mechanism.
- 26: **4. Verify Reactivation**
- 27: a. Query the ledger for the status of the DID.
- 28: b. Confirm that the DID document now reflects the ACTIVE state.

This complete procedure guarantees the legitimacy of transmissions, the integrity of the channel, and the traceability of the sender. The technical flowchart of the process is shown in Fig. 7. Once authenticated, the device can transmit its data through the satellite channel. If its access needs to be suspended, the document associated with its Alias ID is updated with an empty document. This mechanism effectively revokes the identity without deleting the root DID and facilitates its subsequent reactivation by restoring the original document. This functionality enables the application of dynamic control policies without compromising the historical traceability of the system [84], which is key in contexts where a flexible identity lifecycle is required.

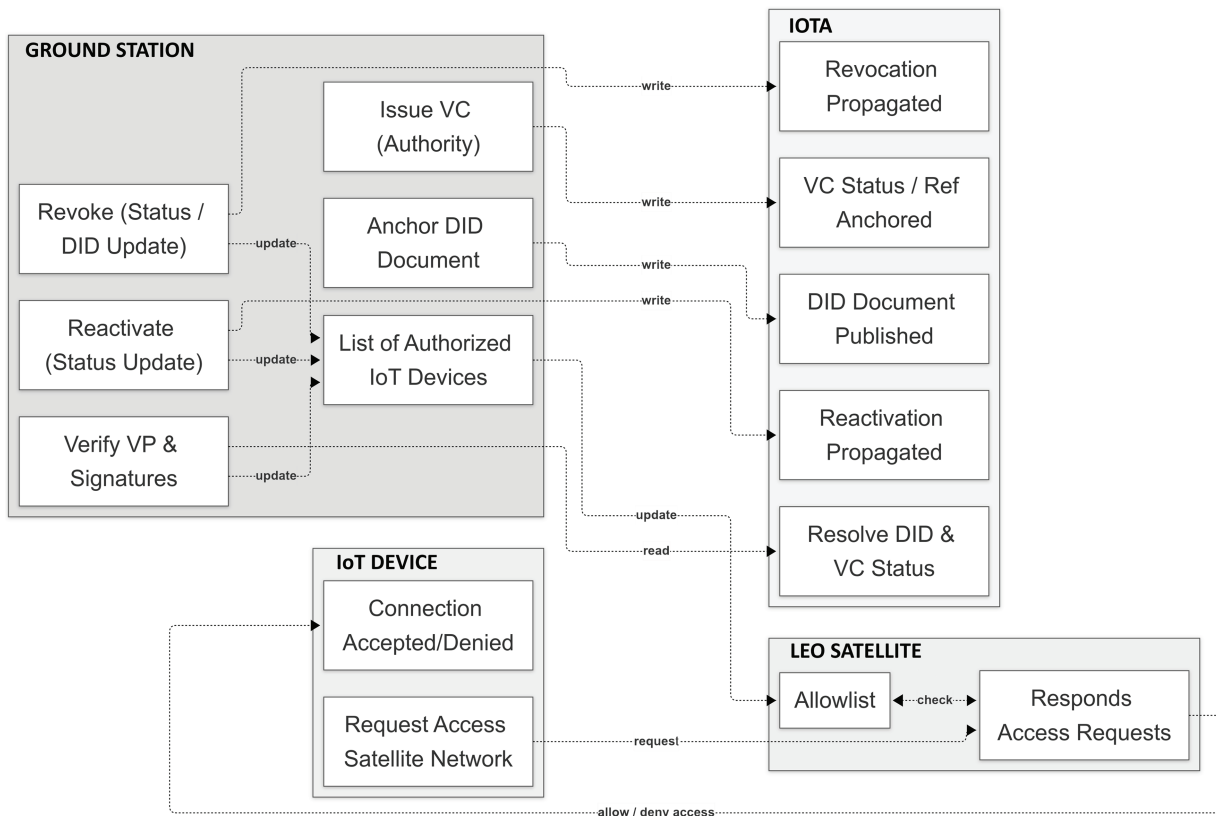


**Figure 7:** Satellite-connected IoT authentication process based on IOTA Identity

### 3.3 Experimental Design and Metrics

The experimental setup developed in this work simulates the connection between a ground station and the IOTA Tangle to carry out tasks such as resolving, deactivating, and reactivating DIDs associated with IoT devices. All tests were conducted using a computer connected to a node in the Shimmer Testnet, which serves as the official public testing network for the IOTA protocol. Shimmer is not a simplified or emulated system; rather, it operates under the same core principles, data structures, and consensus logic as the main IOTA Tangle. This architectural parity ensures that the authentication operations evaluated in the testnet reflect the same execution logic as in the production network. Although it operates under test conditions, Shimmer shares the DAG architecture, validation logic, and DID management protocols with the main Tangle. Consequently, while the measurements obtained accurately reflect the essential behavior of the distributed ledger infrastructure, they may not fully capture the performance characteristics observed in a production network. Shimmer maintains a smaller and less geographically distributed set of nodes, often hosted on non-production-grade hardware and subject to variable maintenance cycles. Its validator and coordinator nodes operate under experimental loads, which can cause greater fluctuation in transaction throughput and message propagation times. As a result, absolute latencies in Shimmer, for example, DID resolution, deactivation, or reactivation times, may be slightly higher and exhibit greater variance than those expected in the main network. In a production-grade Tangle deployment, node density is higher, peer connections are more stable, and the infrastructure is optimized for low-latency operation at scale. Consequently, the same authentication workflows would likely benefit from reduced average execution times and improved stability in time-sensitive operations, particularly under high device concurrency or in geographically dispersed IoT deployments. For this reason, the performance results obtained in Shimmer should be interpreted as a conservative baseline: the relative ordering and proportionality of the measured times remain representative. At the same time, actual production deployment would be expected to yield equal or better performance under equivalent operational conditions. To assess the technical feasibility of the proposed system, three main metrics were defined to quantify the performance of the decentralized authentication process: DID resolution time, DID deactivation time, and DID reactivation time. The delay in resolving a DID was calculated from the moment the resolution function is executed, passing the DID alias as input, to the instant when the Tangle returns a response regarding the status (active/inactive) of the DID. For deactivation, the metric corresponds to the time elapsed between the execution of the deactivation function and the receipt of confirmation from the Tangle that the deactivation has been processed. Reactivation time is similarly measured from the execution of the respective function until confirmation that the DID is once again active. The scale of the experiment considered a network of 100 simulated IoT devices, chosen as a representative scenario for satellite constellations with low IoT device density and consistent with the operational capacity anticipated for initial LEO deployments. This configuration provides a realistic and computationally feasible environment for evaluating identity management operations under the constraints imposed by satellite revisit windows. The selection of metrics and the choice of the device from which interactions with the Tangle are made to manage credentials respond directly to the operational requirements and intrinsic limitations of satellite IoT networks, characterized by restricted link availability, limited processing capacity on the satellite, and short communication windows. Furthermore, the relevance of these metrics was reinforced by comparison with satellite revisit times calculated in MATLAB simulations, which determine how frequently a device, whether an IoT node or a ground station, can establish an uplink. This assessment verifies that permission management operations in the Tangle can be completed within the available connectivity window, ensuring the consistency, reliability, and robustness of the proposed identity management system.

### 3.4 Energy Consumption Measurement Method for DID Operations on IOTA

This work investigates the energy efficiency of IOTA Tangle transactions in the context of DIDs and their associated operations. The analysis focuses on the following message types, as defined by the W3C DID and VC standards:

- DID creation (onboarding of new identities)
- Verification method creation (binding cryptographic material to DIDs)
- Credential revocation (recording the invalidation of issued credentials)
- Credential verification (proving the authenticity of issued credentials)
- Verifiable presentation verification (validating claims shared by an identity holder)

Within the IOTA framework, each of these operations is represented as a message anchored in the Tangle. Following the methodology recommended by the IOTA Foundation, the energy consumed per message is computed as (1)

$$E(x) = \frac{P_{\text{total}}(x) - P_{\text{rest}}}{x} \quad (1)$$

where  $P_{\text{total}}(x)$  denotes the measured power consumption at a throughput of  $x$  DID-related messages per second, and  $P_{\text{rest}}$  represents the idle power consumption of the device [85].

While the present work focuses on latency and operational timing metrics, energy consumption is a critical factor in deploying authentication mechanisms on resource-constrained IoT devices. In this regard, IOTA's Tangle offers structural advantages over conventional blockchain-based systems [48]. The absence of mining and the use of a lightweight tip-selection algorithm reduce the computational demand during transaction validation, which in turn lowers instantaneous power draw [86]. Although no direct energy measurements were performed in this work, these architectural characteristics suggest that the authentication process described here would require fewer processor cycles and less active time compared to blockchain frameworks employing Proof-of-Work or other computationally intensive consensus mechanisms. This lower processing load is particularly relevant in satellite-IoT scenarios with strict duty cycles and limited energy budgets. As future work, we plan to extend the experimental methodology to include empirical energy profiling on representative low-power IoT hardware, enabling a quantitative comparison between Tangle-based and blockchain-based authentication processes. From a network-level perspective, the number of satellites in a constellation can indirectly influence the energy profile of authentication. Higher satellite densities generally reduce revisit times and improve link availability, potentially lowering the energy cost per authentication by minimizing idle or retry periods. Conversely, more frequent handovers between satellites may introduce additional signaling overhead, increasing instantaneous energy usage during these transitions. Quantifying these trade-offs will require experimental campaigns under varying constellation sizes and link conditions, which we identify as a complementary line of future work to the empirical energy profiling described above.

### 3.5 Scalability Considerations

The scalability of the proposed authentication framework must be assessed in terms of its ability to accommodate increasing numbers of IoT devices, higher concurrency of authentication requests, and the dynamic topology imposed by LEO satellite constellations. Unlike blockchain-based ledgers that depend on sequential block formation and proof-of-work mechanisms, the Tangle enables parallel transaction validation without a centralized bottleneck. This structural property provides a favourable scaling trajectory, as verification load can be distributed across multiple nodes without degrading consensus finality times.

From a functional perspective, the per-device computational load for DID resolution, VC issuance, and verification remains constant with network growth, due to the algorithmic complexity of the employed cryptographic primitives and the absence of mining [48]. Consequently, the principal scalability constraint shifts from computational overhead to communication scheduling within satellite contact windows. In large-scale deployments, simultaneous uplink requests during brief visibility periods can saturate the available link budget, resulting in queuing delays. This effect can be mitigated through distributed ground station coverage, opportunistic scheduling, and prioritization strategies that allocate bandwidth according to authentication urgency. From an architectural perspective, scalability can be enhanced horizontally by increasing the number of verifier nodes connected to the Tangle through geographically dispersed ground stations. This approach reduces contention during peak demand and minimizes latency by allowing authentication requests to be processed at the node with the nearest ledger access. Vertical scalability, improving the processing capabilities of individual verifier nodes, can be achieved by optimizing signature verification routines, employing hardware acceleration for cryptographic operations, and adopting high-throughput networking stacks. Temporal scalability must also be considered in relation to satellite revisit cycles. As the number of satellites in a constellation increases, the effective revisit time decreases, distributing the authentication load over more frequent but shorter contact intervals. While this can reduce average queue depth, it may also introduce additional handover signalling, which requires lightweight session continuity protocols to prevent redundant authentications. Although the present work does not experimentally validate scalability at production-level network sizes, the architectural properties of the Tangle and the proposed distribution of verifier nodes indicate that the system can maintain stable performance in deployments exceeding thousands of active IoT devices [61].

### 3.6 Analytical Basis for Estimating Latency from Throughput

This analysis follows the fundamental latency-throughput relation [87], expressed as

$$h = \frac{r}{\lambda} \quad (2)$$

where  $h$  is the average confirmation latency,  $r$  is the number of visible tips, and  $\lambda$  is the throughput measured in messages per second. This expression provides the foundation for linking transaction load and validation delay within the IOTA Tangle. To account for the effects of network congestion as throughput increases, we adopt a simplified extension of the baseline relation. In this formulation, latency is expressed as

$$h(\lambda) = h_0 \left( 1 + \frac{\lambda}{\lambda_{\max}} \right) \quad (3)$$

where  $h_0$  represents the baseline propagation and computation time per transaction, and  $\lambda_{\max}$  denotes the approximate capacity of the network. This approach maintains consistency with the steady-state assumption at low loads, while reflecting the growth in latency as throughput approaches capacity. Given that DID operations are dominated by resolution messages, while deactivation and reactivation remain relatively rare, the workload is modeled as homogeneous in transaction processing cost.

#### *Reducing Revocation Latency through Local Mechanisms and Prevalidation*

To reduce the latency of effectively turning off devices with intermittent contacts, we integrate two additional local mechanisms, kept consistent with the IOTA Identity source of trust:

- A temporary allowlist stored onboard.
- Pre-validation using short-lived capability tokens.

The standard revocation process updates the device state in the Tangle, recording the revocation in a persistent and immutable manner [88]. However, this operation depends on the required confirmation depth and the propagation times  $\Delta_{\text{prop}}$  of the distributed infrastructure. To shorten the exposure interval before the revocation is crystallized in the DLT, a temporary update of the onboard allowlist is used, which immediately excludes devices for which revocation has been requested, even if it has not yet been confirmed in the Tangle. This strategy does not require an explicit denylist; rather, it produces a temporarily reduced set of authorized devices, which is functionally equivalent to denying access to excluded devices. Formally, if  $W_t$  is the allowlist at time  $t$ , then

$$W_{t+\varepsilon} = W_t \setminus D_r \quad (4)$$

where  $D_r$  is the set of devices whose revocation is being confirmed. Thus, the temporal allowlist  $W_{t+\varepsilon}$  defines effective access until the revoked state stabilizes in the Tangle

$$\lim_{t \rightarrow t^*} W_t = W_{\text{Tangle}} \quad (5)$$

where  $t^*$  is the time at which the update in the Tangle reaches probabilistic completion according to the confirmation policy and distributed propagation. This mechanism enables the secure and agile retirement of revoked devices, mitigating the risks associated with the transient interval between the revocation request and its consolidation in the network. The implementation requires dynamic and synchronized management between satellites, ideally leveraging Inter-Satellite Links (ISLs) to propagate the new allowlist state to the entire constellation. Once the revocation is definitively confirmed in the Tangle, the local allowlists are resynchronized with the authorized global state, eliminating the temporary modification and restoring consistency with the Tangle. Pre-validation is articulated through short-lived signed capability tokens.

$$C = (\text{DID}, \text{scope}, \text{nbf}, \text{exp}, \text{nonce}, \text{sig}) \quad (6)$$

to holders that have passed ledger-based verification. Satellites only accept traffic when a valid  $C$  accompanies the DID, enabling local expiry of access without requiring a deactivation round-trip to the ledger. Tokens are bound to scope (e.g., service, bitrate) and windowed by (nbf, exp) to constrain replay. Operationally, these overlays change the effective latency model to

$$T_{\text{deact}}^* = \min \{ T_{\text{ledger}}^{\text{deact}} + W + T_{\text{onboard\_update}}, T_{\text{overlay}} \} \quad (7)$$

where  $T_{\text{overlay}}$  is the time to enforce  $L_t$  or to observe token expiry, typically on the order of seconds, and independent of  $W$ .

### 3.7 Task-Offloading and Response Rate

Task-offloading in the proposed satellite-IoT authentication framework refers to the delegation of computationally intensive operations to avoid overloading resource-constrained devices, such as LEO satellites or IoT devices. Tasks such as DID creation, cryptographic signature verification, revocation list checking, or credential status validation are transferred from resource-constrained LEO satellites or IoT devices to ground stations for processing. In terms of performance, the integration of task offloading has a direct impact on the response rate. At the device level, eliminating the need to execute computationally intensive cryptographic routines reduces active processor cycles and can lower instantaneous power consumption. However, in LEO satellite environments with intermittent connectivity and short contact windows, the net latency benefit depends on whether the local processing time saved outweighs the additional communication delay required to transfer intermediate data to the processing node. This trade-off is exacerbated when considering satellite

handovers or high network load, where queuing delays at the gateway or ground station can partially offset the benefits derived from reduced on-device computation. While this work focuses on operational times measured in a direct execution scenario, the experimental results provide relevant boundary conditions for future offloading evaluations. Specifically, the observed DID resolution and wake-up times establish an upper bound on acceptable end-to-end latency when offloading is employed. In contrast, the variability in deactivation times suggests that stringent buffering and retry policies would be required to ensure reliability in offloaded execution. Future work should experimentally quantify these trade-offs by simulating offloading with different link availabilities, constellation sizes, and concurrent authentication loads, allowing for a rigorous evaluation of its impact on both latency and system scalability in the context of the proposed architecture [89].

### 3.8 Security Model and Cryptographic Assumptions

The authentication protocol  $\Pi$  is analyzed under a computational security viewpoint with security parameter  $\lambda$ . The system comprises holders and issuers of verifiable credentials, a verifier running at the ground station or satellite gateway, and the IOTA Tangle, which is used as a tamper-evident, append-only substrate for decentralized identifiers and credential metadata. Trust boundaries are explicit: end devices and ground stations are assumed to execute the prescribed protocol without malicious deviations, private signing keys remain confidential on their respective endpoints, and the Tangle provides eventual consistency with probabilistic finality once a confirmation threshold is reached. The cryptographic layer relies on standard digital signatures with existential unforgeability under chosen-message attacks, as well as collision-resistant hash functions, for commitments and message digests. Verifiable presentations are bound to the holder's key material and include freshness material, such as nonces and expiration times, transported in compact encodings (e.g., JWT). Under these assumptions, the advantage of any probabilistic polynomial-time adversary in producing a valid presentation for an identity it does not control is negligible in  $\lambda$ , as such an attack reduces to forging a signature or breaking the binding between a DID and its public key, both of which contradict the stated hardness assumptions [90]. Freshness data ensures that replayed presentations are rejected outside their validity window. Collisions in nonces are negligible for appropriate entropy and window sizes, and verifier-side acceptance policies bound clock skew. Integrity of credential material follows from signature verification at the verifier and the immutability guarantees of the ledger; any bit-level deviation in credential payloads or ledger-anchored descriptors is detected due to verification failures or hash mismatches. Ledger semantics are modeled as an eventually consistent DAG with probabilistic finality. Let  $k$  denote the confirmation depth required by the verifier and  $\Delta_{\text{prop}}$  the upper bound on propagation under nominal conditions. Once a deactivation update is issued at time  $t_0$ , the probability that a resolver observing the ledger at or after  $t_0 + k \Delta_{\text{prop}}$  still obtains the pre-deactivation state is negligible in  $\lambda$ ; this follows from the tamper-evident nature of the Tangle and the monotonicity of confirmations beyond the chosen depth. The safety of revocation, therefore, remains after the confirmation horizon. In contrast, the interval preceding finality is a race condition explicitly acknowledged in our operational model and treated as a transient risk window. The intermittent availability of links in LEO scenarios constrains liveness and timeliness. Let  $W$  denote the random waiting time to the next usable contact and  $T_{\text{ledger}}$  the ledger-side service time measured in our experiments. The effective latency perceived by the system is

$$T^* = T_{\text{ledger}} + W + T_{\text{onboard\_update}} \quad (8)$$

This decomposition separates cryptographic service time, which is under protocol and infrastructure control, from link-induced delay, which is governed by orbital dynamics and scheduling. The analysis shows that the ordering of operations is preserved across conditions; deactivation remains the most sensitive

phase because its effect must be recognized across verifiers only after ledger finality, while activation and resolution are primarily bounded by local verification and read-only queries. Privacy considerations arise from metadata in presentations and ledger lookups [91]. The protocol adopts minimal disclosure consistent with verifiable credential practice, avoiding the publication of attribute values on-chain and limiting ledger usage to identifiers and proofs necessary for verification. Residual linkability may occur through correlation of repeated lookups or timing side channels; such risks are mitigated operationally by caching policies at verifiers and, when required by the application, by selective disclosure techniques. A full privacy proof in a formal model is identified as future work and falls beyond the empirical scope of this work. The stated guarantees are contingent on the correctness of cryptographic implementations, the confidentiality of private keys on endpoints, and the ledger's finality policy. Side-channel resistance, compromise of endpoint keys, and active subversion of verifiers are not modeled here and would require a different class of assurances, typically involving hardware roots of trust and system-level attestation. Likewise, the derivations do not claim bounds on energy or radio-layer leakage, which are orthogonal to the protocol's cryptographic core. Within these boundaries, and under the standard unforgeability and collision-resistance assumptions, the authenticity, integrity, replay resistance, and post-finality revocation safety of II hold with negligible adversarial advantage.

#### 4 Results

To obtain viable statistical results on the time required to resolve, deactivate, and reactivate DIDs, an experimental infrastructure based on 100 simulated IoT devices was implemented. To this end, 100 DIDs were created. The test consisted of executing 100 DID resolutions, one for each DID created. 100 DID deactivations were also executed for each of the created and resolved DIDs. 100 DID reactivations were also executed for each of the deactivated DIDs. To this end, the official IOTA Identity libraries were used on the Shimmer Testnet. Table 4 lists the main statistics obtained for each of the three metrics evaluated. In addition to the table, the data can also be visualized in Fig. 8, which presents the comparative boxplots for these metrics.

**Table 4:** Statistics for resolution, deactivation, and reactivation time

| Statistic     | Resolution | Deactivation  | Reactivation |
|---------------|------------|---------------|--------------|
| Minimum       | 123.0      | 4222.0        | 123.0        |
| Maximum       | 433.0      | 87,536.0      | 656.0        |
| Range         | 310.0      | 83,314.0      | 533.0        |
| Mode          | 135.0      | 9777.0        | 133.0        |
| Mean          | 153.3      | 26,080.7      | 155.5        |
| Median        | 139.0      | 19,930.00     | 141.0        |
| Variance      | 2320.3     | 312,873,278.2 | 4570.1       |
| St. Deviation | 48.2       | 17,688.2      | 67.6         |
| Skewness      | 3.7        | 1.4           | 5.2          |

Note: All values are in milliseconds.

Regarding resolution time, a mean value of 153.68 ms and a median of 139.00 ms were observed, with a standard deviation of 48.17 ms. The distribution exhibits positive skewness (3.72), indicating the presence of longer outliers, although they are concentrated within a narrow range. This suggests that the operation is highly consistent and suitable for systems requiring predictable latencies.

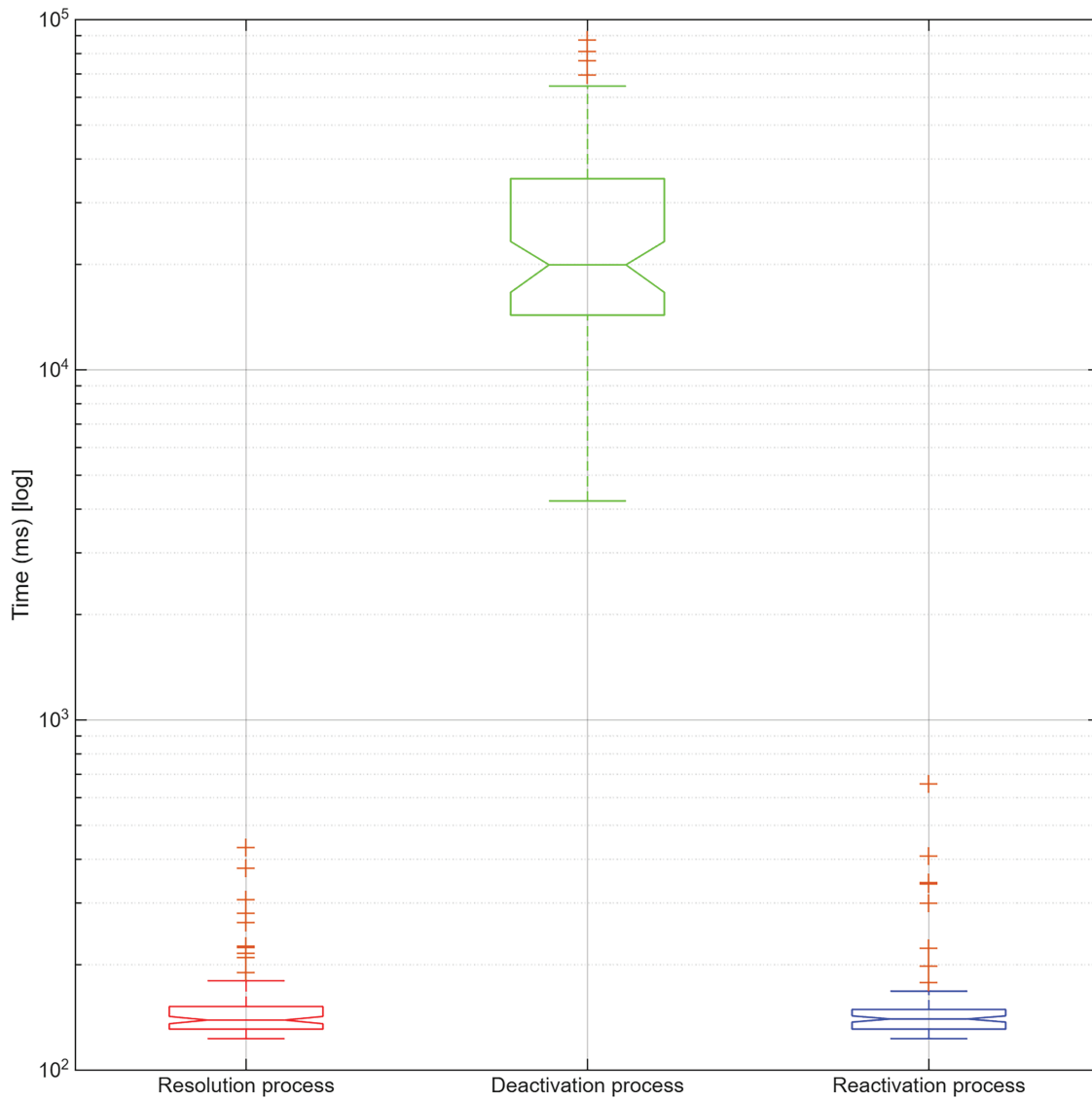


**Figure 8:** Comparison of time distributions

In the case of deactivation, the system showed greater variability, with a mean time of 26,080.72 ms and a standard deviation of 17,688.22 ms. The median was 20,308.00 ms, and maximum times of up to 87,536.00 ms were recorded. This dispersion is attributed to internal Tangle processes related to resource release and update propagation. However, the skewness analysis (1.36) reveals that most operations were executed faster than average, albeit with a higher dispersion. Reactivating a DID displayed very similar behavior to the resolution process, with an average time of 155.52 ms and a median of 141.00 ms. The standard deviation was 67.61 ms, while the skewness reached 5.22 ms, indicating a strong bias toward low values with a few extreme cases. These results confirm that restoring a previously deactivated identity can be performed quickly, allowing device reauthentication without significant delays.

The statistical characterization of the authentication operations provides further insight into the system's performance. For credential resolution, the average time was 153.7 s, with a 95% confidence interval of [144.1, 163.3]. The hypothesis test confirmed that the mean is significantly below the 600 s reference threshold

( $p < 0.0001$ ). Similar behavior was observed for credential reactivation, with an average of 155.5 s and a 95% confidence interval of [142.0, 169.0], also significantly lower than 600 s ( $p < 0.0001$ ). These results demonstrate that both resolution and reactivation can be consistently executed within the temporal margins imposed by LEO satellite revisit windows. In contrast, credential deactivation exhibited a markedly higher variability, with an average time of 26,080.7 s and a 95% confidence interval of [22, 552.9, 29, 608.6]. In this case, the null hypothesis that the mean deactivation time is greater than or equal to 600 s could not be rejected ( $p = 1.0000$ ). This dispersion indicates that, although the mechanism is functional, its performance is not yet aligned with the temporal requirements of scenarios demanding rapid access revocation. Consequently, deactivation emerges as the most critical operation to be optimized in order to ensure suitability for deployment in high-security IoT satellite environments.

In parallel, a simulation was developed to estimate LEO satellite revisit times at different latitudes, using a Walker Star-type orbital configuration with an altitude of 400 km and an antenna aperture of  $120^\circ$  [92]. Fig. 9 presents the results obtained, which illustrate how the revisit frequency varies with latitude and the number of satellites in the constellation. At high latitudes, where coverage is more frequent, revisit times decrease significantly as the number of satellites increases. In the case of dense constellations (100 or more satellites), minimum times of up to 36 s were reached at latitudes near the poles, while at low latitudes, the values exceed 11 h with reduced constellations. Comparing these times with those obtained for operations on the Tangle confirms that both identity resolution and reactivation can be completed within the period the device is in satellite coverage.

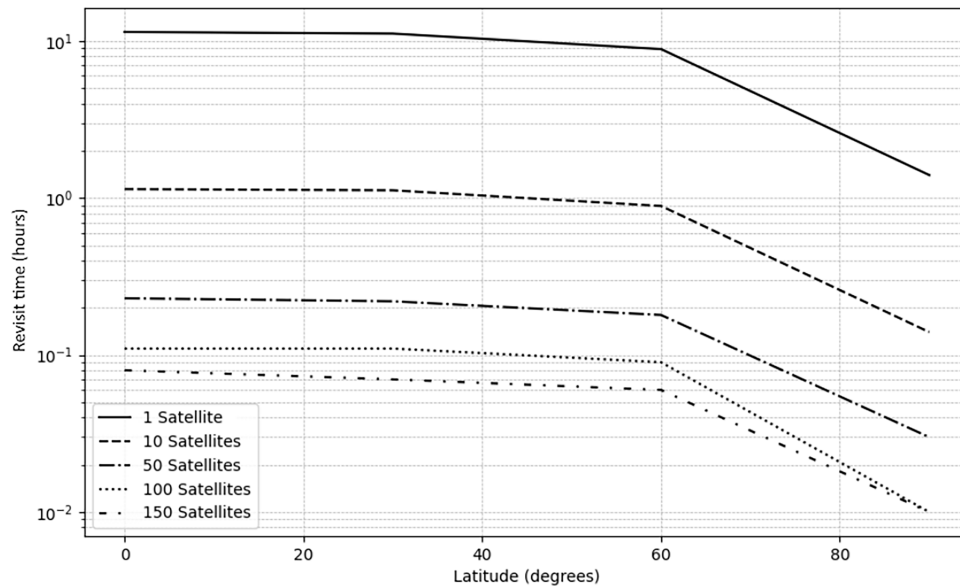


**Figure 9:** Satellite revisit time as a function of latitude

#### 4.1 Latency and Variance Considerations

The end-to-end latency measured for IOTA-based authentication in this work is 155.5 ms for revocation and 153.3 ms for reactivation events (see Table 4). These stable and bounded values are primarily attributed to optimizations in the decentralized identity resolution process within the Tangle, which validates references on a distributed ledger more efficiently, completing the authentication protocol with less overhead compared to centralized systems. In contrast, deactivation times exhibit greater variability, with occasional values that can exceed the activation latency, largely influenced by network propagation delays, temporary congestion

in information selection from the Tangle, and the level of confirmation required for a deactivation to be finalized. These factors are particularly impactful in scenarios where device state changes are infrequent but must be executed quickly for security reasons. Potential optimizations to mitigate these observations include using credential state caching to avoid redundant lookups, dynamically adjusting commit depth based on transaction criticality, and exploring parallel transaction submission to reduce network latency. Future work will evaluate these techniques under realistic LEO satellite link conditions, where intermittent connectivity could amplify both average latency and its variability.

#### 4.2 Energy Consumption Per DID Operation as a Function of Throughput

The experimental environment was configured to emulate a low-power edge node, modeled after a Raspberry Pi 4 or an equivalent platform, serving as an identity node within a decentralized IoT or industrial infrastructure. Measurements were performed under two workload conditions: 100 messages per second, corresponding to a low-intensity identity workload, and 1000 messages per second, representing a high-throughput operational context. A linear interpolation between these measurement points was subsequently employed to estimate energy consumption across intermediate and higher throughput levels. The results indicate that the energy cost per DID-related message decreases notably as the message rate increases. At 100 messages per second, each DID operation (e.g., DID creation or credential verification) requires approximately 0.05 J/message. In contrast, at 1000 messages per second, the energy cost declines to 0.015 J/message, with the model predicting an asymptotic lower bound of approximately 0.011 J/message at higher loads. Fig. 10 summarizes these findings, illustrating that the energy per operation declines with increasing throughput due to the amortization of system overhead. At low message rates, baseline consumption constitutes a significant portion of the total energy demand. However, as throughput increases, the relative impact of this baseline diminishes, thereby enhancing overall system efficiency.

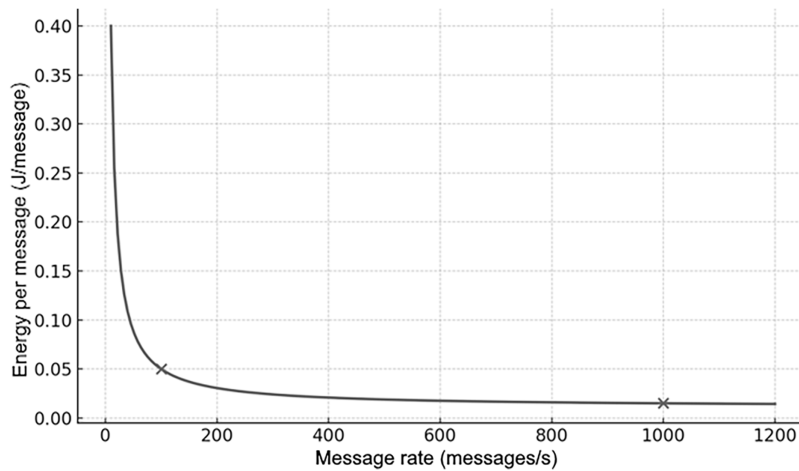


**Figure 10:** Energy consumption per DID-related message as a function of throughput in the IOTA tangle

#### 4.3 Estimated Latency-Throughput Profile for DID Resolution Messages

The baseline latency parameter was set to  $h_0 = 153.3$  ms as reported in Table 4. Using this value within the extended congestion model and assuming a nominal network capacity of  $\lambda_{\max} = 1000$  msg/s, the resulting latency curve, as shown in Fig. 11, was computed across throughput values ranging from 1 to 2000 messages per second.

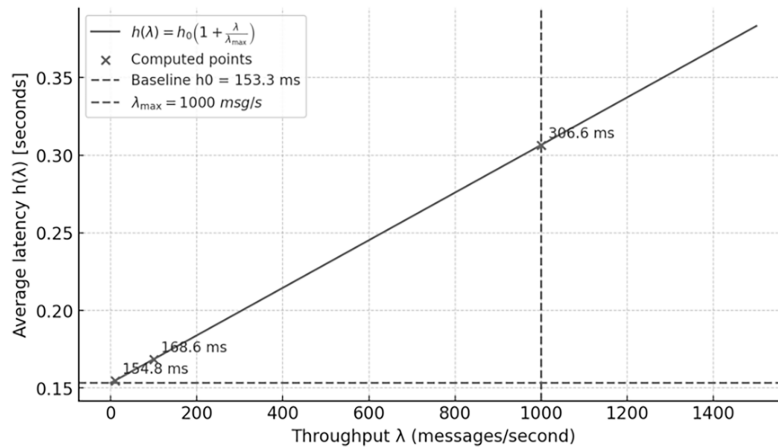


**Figure 11:** Estimated average latency vs. throughput for did resolution messages in the IOTA tangle

The resulting graph shows that latency remains close to the baseline under light load conditions, indicating that propagation and computation time dominate performance in this regime. As throughput increases, latency gradually grows until it approaches the capacity threshold, where the rise becomes more pronounced. Beyond the assumed capacity, the curve continues to increase linearly, reflecting congestion-driven degradation of performance.

## 5 Discussion

Analysis of the results shows that the distributed authentication system based on IOTA Identity can operate efficiently in intermittent satellite connectivity environments. Resolution and reactivation times consistently remained below 160 ms, thus meeting the minimum standard of 400 ms in LEO communications [93], even in the most extreme cases recorded during testing, enabling rapid identity management of IoT devices without generating significant delays in data transmission. This feature is especially relevant in scenarios where devices are subject to constant movement or limited coverage. Recent publications highlight the limitations of low latency in satellite IoT networks, particularly in ensuring continuous device authentication, especially in high-mobility environments and areas with limited satellite coverage [94]. In contrast, the deactivation time showed considerable variability, with maximum values exceeding 80 s. While these results remain manageable for many applications, they reveal the need to improve identity revocation mechanisms in the Tangle to ensure the consistency of information from authorized devices to the satellite infrastructure. The observed dispersion suggests that performance in this operation is influenced by factors related to storage management and update propagation in the distributed network. This behavior has also been observed in previous research on blockchain-based systems, which suggests that revocation operations can be affected by network saturation or peak processing demand [69]. The reactivation time showed very favorable performance, allowing device access to be restored almost immediately once the DID document was resolved. This capability is useful in applications that require frequent activation and deactivation cycles, such as periodic data acquisition systems or low-power devices operating in intermittent mode. The rapid reactivation process minimizes the impact of interruptions in the authentication channel and facilitates more flexible access management [95], highlighting the importance of rapid credential restoration in IoT networks. This emphasizes that it minimizes interruptions in the authentication of devices that require repeated activation and deactivation. From an operational perspective, these times must be analyzed in relation to the connectivity and revisit intervals imposed by satellite orbits. As evidenced in the orbital simulation, revisit times vary depending on latitude and constellation size, being shorter at high latitudes and

with a greater number of satellites. In representative configurations with 100 or more satellites, minimum times of up to 36 s were observed, implying that even the slowest system operations (such as deactivation) can be completed within the inter-revisit window. This validates the feasibility of integrating the proposed system into real satellite networks, provided that design policies are considered to avoid critical revocation operations during the shortest link times [92]. The energy consumption of DID operations behavior suggests that IOTA-based identity management becomes increasingly energy-efficient as it scales. In large-scale IoT ecosystems, where thousands of devices regularly generate and verify credentials, the marginal energy cost per transaction approaches negligible levels. Similarly, in industrial infrastructures requiring frequent credential revocations and verifiable presentation checks, the system is capable of sustaining high transaction volumes while maintaining low per-operation energy expenditure. Overall, the results confirm that IOTA Identity constitutes a viable technical alternative to centralized or blockchain-based models for authenticating IoT devices in satellite environments. However, areas for improvement are identified, such as optimizing the deactivation process and evaluating performance under different orbital configurations or device densities. These issues are addressed in the Limitations and Future Research section.

The results highlight the sensitivity of latency in the IOTA Tangle to network load. At low to moderate throughput, the system operates efficiently, with latency remaining close to the propagation baseline. However, as the offered load approaches the network's capacity, the latency nearly doubles, which could significantly affect the responsiveness of DID resolution operations. This behavior suggests that while the Tangle can handle substantial message volumes without immediate performance loss, sustained operation near or above capacity risks producing delays that could undermine the usability of latency-sensitive applications. Future work could refine this model by distinguishing resolution from other DID message types and by calibrating  $\lambda_{\max}$  using empirical throughput data from real deployments.

### 5.1 Comparative Analysis between DAG-Based Validation and Block-Based Consensus

Authentication workflows that rely on a ledger incur a ledger-side component whose structure depends on the underlying consistency mechanism [48]. In block-based systems with fixed block interval  $B$  and confirmation depth  $k$ , any decision that depends on a ledger write or observing a state change must satisfy a timing path with a lower bound.  $L_{\text{net}}$  accounts for propagation and queuing on the publication path, while  $L_{\text{verify}}$  captures cryptographic verification and local processing

$$L_{\text{block}} \geq k B + L_{\text{net}} + L_{\text{verify}} \quad (9)$$

This bound is structural: even under negligible propagation and abundant processing capacity, the block cadence imposes a floor proportional to  $kB$  on ledger-mediated operations. The Tangle validates transactions asynchronously and does not aggregate them into globally paced blocks. Confirmation depth is expressed as a policy on confidence, which depends on cumulative weight, local topology, and propagation rather than on a fixed temporal cadence [96]. For read-dominant operations such as DID resolution and credential reactivation checks, the absence of a block-interval floor eliminates the  $kB$  term in (9), leaving the ledger-side latency primarily driven by propagation and local verification. This explains why the measured service times for resolution and reactivation remain below 160 ms under non-congested conditions in our setup. For write-dominant operations such as deactivation, the variance is higher because verifiers must recognize the effect after a policy-defined confidence horizon; in the Tangle, this horizon is governed by propagation and tip selection dynamics rather than by a fixed block cadence, which makes the variance sensitive to transient network conditions [97].

### 5.2 Scalability beyond 100 Devices: Window-Limited Capacity, Concurrency, and Throughput

Scalability in satellite-IoT deployments is governed jointly by ledger-side service time and the temporal structure of contact windows. Let  $T_{\text{total}}$  denote the mean service time per authentication request measured at the verifier (including resolution and, when applicable, revocation handling), and let  $W$  be the duration of a satellite-ground contact window. The maximum number of *sequential* authentications that can be completed within a single window satisfies the window-limited capacity relation.

$$N_{\text{win}} \approx \frac{W}{T_{\text{total}}} \quad (10)$$

When multiple devices attempt authentication concurrently, arrivals during a window can be modeled by an aggregate rate  $\lambda$  and served by  $m$  parallel verifier instances distributed across ground stations. Stability requires  $\rho = \lambda T_{\text{total}}/m < 1$ . Under stability, the expected number of completions per window is limited by both processing and link capacity. If  $C_{\text{uplink}}$  denotes the uplink capacity allocated to authentication traffic and  $S_{\text{auth}}$  the average payload per authentication, an upper bound on the effective throughput over the window is. The number of completions satisfies  $N_{\text{eff}} \leq R_{\text{eff}} W$ . This bound captures the two primary bottlenecks: verifier-side processing and the fraction of the radio link budget dedicated to authentication.

$$R_{\text{eff}} \leq \min \left( \frac{m}{T_{\text{total}}}, \frac{C_{\text{uplink}}}{S_{\text{auth}}} \right) \quad (11)$$

For constellations exceeding 100 devices or for dense IoT scenarios, the contact schedule modulates concurrency by compressing request arrivals near pass edges. If burstiness concentrates arrivals into a subinterval of width  $\omega \leq W$ , the instantaneous arrival rate scales as  $\lambda_{\text{max}} \approx N_{\text{arr}}/\omega$ , where  $N_{\text{arr}}$  is the number of devices seeking authentication in that window. Meeting  $\rho < 1$  under such bursts requires either increasing  $m$  through geographically distributed verifiers, spreading arrivals by policy (e.g., randomized backoff across the window), or reducing  $T_{\text{total}}$  via caching and pre-validation. The asynchronous validation properties of the Tangle avoid a block-interval bottleneck on the consensus side, which prevents the emergence of a global cadence term in (11) as device populations grow. Deactivation at scale is affected by the requirement to observe a state change due to revocation. If a policy imposes a confirmation horizon  $T_{\text{conf}}$  on revocations, the service time for deactivation includes a term that is insensitive to verifier parallelism. Local overlays limit the exposure of this term by enforcing revocation immediately and reconciling at the next contact. In practice, combining distributed verifiers to increase  $m$ , admission control to cap burstiness, and overlays to shrink the dependence on  $T_{\text{conf}}$  yields a capacity region in which the fraction of devices successfully authenticated or revoked within each window remains near one even as populations scale. The empirical service times measured in this work define the processing term in (10) and (11), and the extended analysis outlines how these times are projected to high-density deployments without relying on external benchmarks.

Local overlays reduce both the mean and variance of the effective deactivation time by removing the dependency on the wait time  $W$  until the next contact. When the temporal allowlist is updated on each pass and tokens have short lifetimes,  $T_{\text{overlay}}$  predominates, producing a narrower spread than

$$T_{\text{ledger}}^{\text{deact}} + W \quad (12)$$

Resolution and reactivation remain primarily constrained by the ledger at the ground station, so their relative order of deactivation is preserved while the worst-case queue is shortened.

### 5.3 Limitations and Future Work

This work establishes a feasibility baseline for decentralized authentication in satellite-LEO-IoT environments using IOTA Identity. However, several limitations restrict the scope of the findings. Measurements focus on ledger-side service times and protocol responsiveness under controlled conditions on the Shimmer Testnet, which is functionally aligned with Tangle but operates in a non-productive environment. Although this network is functionally equivalent to the IOTA Tangle, it does not reproduce the conditions of a production deployment in terms of sustained load, long-term resilience, or exposure to adversarial behavior. Consequently, while the obtained results are valid to assess functional feasibility, future validation on a production-grade network is required to confirm robustness under operational stress. The intermittent satellite connection was analytically modeled rather than emulated on the physical link, and experiments focused on single-device sequences without concurrent access pressure. These limits imply that the reported latencies should be interpreted as reference values for the cryptographic and ledger layers, not as end-to-end operational limits on active LEO links.

The deactivation path exhibits greater variance than resolution and reactivation, a behavior consistent with the propagation and confirmation depth in a DAG ledger, as well as the reconciliation time of updates between verifiers. When the effective latency is decomposed as

$$T^* = T_{\text{ledger}} + W + T_{\text{onboard\_update}} \quad (13)$$

The random waiting component  $W$  associated with the next usable contact window between the satellite and the ground station that will update the list of devices allowed in the system dominates the dispersion in LEO scenarios, while  $T_{\text{ledger}}$  remains comparatively stable. This explains the sensitivity of deactivation under scattered passes and congested spikes and motivates architectural mechanisms that reduce the dependence on immediate ledger observation between contacts, while preserving eventual consistency. Lightweight consensus can further reduce deactivation delay when multiple ground stations or gateway verifiers are available. DAG-compatible leaderless quorum formation on revocation attempts enables a verifier to enforce a decision after reaching a local threshold and before global finality is achieved, with subsequent anchoring to the Tangle for tamper-evident auditing. The trade-off is explicit: increased timeliness in the control plane comes at the cost of a short reconciliation window, during which decisions are locally consistent but globally final. Parameterization of quorum size, timeout, and reconciliation policy should be calibrated based on contact frequency and expected network load. Edge intelligence provides an orthogonal path to reducing end-to-end latency. Deterministic rule sets or lightweight classifiers deployed at the ground station can prioritize credential checks, pre-validate recurring sessions within limited lifetimes, and schedule revocation updates to precede non-critical traffic during short passes. Any inference results remain advisory, with the cryptographic decision anchored to verifiable credentials and presentations. This separation maintains the integrity of the security model while leveraging locality to reduce delay. Resource usage must be limited in memory and compute to maintain compatibility with internal constraints and avoid interference with mission traffic. Scalability with concurrent access requires analysis that transcends single-flow latency. Achievable throughput during a pass is limited by the length of the contact window, the uplink capacity available for update traffic, the size of the credential payloads, the processing budget on the verifying nodes, and the ledger confirmation dynamics under load. Tangle's asynchronous validation properties favor horizontal scaling among multiple verifiers connected via geographically distributed ground stations. Parallel dispatch policies should avoid contention in track selection and ensure fairness between device cohorts. The theoretical capacity derived from the  $T_{\text{ledger}}$  measurement will be complemented by stress tests under concurrent request arrivals to characterize queuing behavior and tail latency. Future validation will address three complementary axes. Hardware-in-the-loop experiments on representative microcontroller nodes

will quantify CPU cycles, active time, and energy per authentication under realistic duty cycles, providing empirical evidence for energy analysis. Link-aware tests with channel emulation and contact scheduling will measure the contribution of  $W$  and the impact of handoffs on both the mean and variance, bridging the gap between analytical and operational behavior. Semi-operational and operational testing with real LEO passes, in collaboration with existing testbeds, will evaluate robustness under real-world channel variability and mixed traffic, and verify that overlay enforcement, lightweight consensus, and edge policies maintain correctness when reconciled with the ledger. The above roadmap preserves cryptographic guarantees of authenticity, integrity, replay resistance, and post-completion revocation security, while focusing on deployment readiness. By combining overlay enforcement for timeliness, quorum-based control for multi-site verifiers, and boundary-aware scheduling with strict resource budgets, the architecture is positioned for pilot deployment, with production-scale validation contingent on upcoming empirical campaigns. An additional line of optimization considers the possibility of optimizing access control within the satellite constellation through the use of ISLs [98], which enable efficient and synchronized updates to the authorized devices on each satellite. Specifically, each satellite maintains a local allowlist of authorized DIDs, stored in orbit to allow or deny access to IoT devices based on their credentials. This allowlist is updated periodically when the satellite establishes communication with a ground station to download cryptographic proofs and relevant information from the Tangle. However, as a complementary improvement or optimization algorithm, we propose implementing direct inter-satellite communication, which would enable rapid and distributed propagation of the updated allowlist throughout the constellation. This way, when a DID is revoked, the information would not have to wait for all the satellites in the constellation to pass over the ground station. Instead, it would be replicated throughout the satellite network via inter-satellite links when the first satellite received the update. This in-orbit distribution of this list ensures that all satellites have the most recent version, minimizing the risk of unauthorized access during periods when a satellite has not yet received updated data from the ground.

Overlays present specific disadvantages in terms of security and privacy. Obsolescence is possible if  $L_t$  expires before the update; to limit risk, artifacts have an expiration date  $\text{exp}$  and are rejected when  $\text{ver}$  is non-monotonic. Update poisoning is mitigated by public keys and satellite signatures, authenticated transport, and replay protection using nonces and sequence numbers. Temporal allowlists can reveal device identifiers; to mitigate this, identifiers are hashed using rotating hashes, and capacity-bound structures are used to prevent enumerability. Capability tokens are short-lived and tied to scope and *nonce* to limit replay and privilege escalation. These overlays preserve the trust and verification semantics of the DID/VC flow, the Tangle maintains authoritative state, while the embedded application provides timely control between contacts. Future work includes a formal analysis of freshness and security under delayed or reordered updates, as well as an empirical evaluation of filter parameters and token lifetimes under different constellation densities.

## 6 Conclusions

This work evaluated, for the first time, the feasibility of an authentication framework for IoT devices in LEO satellite constellations based on IOTA Identity. This framework encompasses distributed identity resolution, deactivation, and reactivation tests, as well as simulations of satellite revisit times. The proposed architecture leverages the DAG-based Tangle to manage decentralized identifiers and verifiable credentials, thereby eliminating the computational overhead associated with mining or block-based consensus. This approach reduces latency and processing demands compared to blockchain-based approaches. Experimental results confirm that credential resolution and reactivation times consistently remain within the operating windows defined by the revisit intervals from LEO satellites to the ground station, from where they update

the list of authorized devices, enabling reliable authentication and credential restoration under intermittent connectivity conditions. Deactivation times showed greater variability, highlighting the need for targeted algorithmic optimization in scenarios with strict security requirements and rapid revocation demands. Tangle's structural properties suggest lower power requirements for resource-constrained devices, a factor particularly relevant in IoT satellite deployments with strict duty cycles. In addition to validating operational feasibility, this work lays the groundwork for pilot implementation in simulated and semi-operational satellite environments, paving the way for future large-scale deployments. The findings underscore both the novelty and practical applicability of DAG-based DLT for secure and scalable IoT authentication in hybrid space-to-ground networks, while defining clear guidelines for optimization prior to production-level deployment. Additionally, the measured end-to-end latency for IOTA resolution and wake-up events remains below 400 ms, which is suitable for the context of LEO satellite communications [93].

**Acknowledgement:** The authors would like to thank Impierce for their support in resolving questions about IOTA Identity.

**Funding Statement:** This work is part of the 'Intelligent and Cyber-Secure Platform for Adaptive Optimization in the Simultaneous Operation of Heterogeneous Autonomous Robots (PICRAH4.0)', with reference MIG-20232082, funded by MCIN/AEI/10.13039/501100011033. This work is partially supported by the Universidad Internacional de La Rioja (UNIR) through the Precompetitive Research Project entitled "Nuevos Horizontes en Internet de las Cosas y NewSpace (NEWIOT)", reference PP-2024-13, funded under the 2024 Call for Research Projects.

**Author Contributions:** The authors confirm their contribution to the paper as follows: work conception and design: D. Bernal, O. Ledesma and P. Lamo; data collection: D. Bernal; analysis and interpretation of results: D. Bernal and O. Ledesma; draft manuscript preparation: D. Bernal, O. Ledesma, P. Lamo and J. Bermejo. All authors reviewed the results and approved the final version of the manuscript.

**Availability of Data and Materials:** The source code used for the tests conducted in this work is available at the following link: <https://doi.org/10.5281/zenodo.16940188> (accessed on 15 September 2025).

**Ethics Approval:** Not applicable.

**Conflicts of Interest:** The authors declare no conflicts of interest to report regarding the present work.

## Glossary

All acronyms that appear in this work are listed below for ease of understanding

| Acronym | Meaning                               |
|---------|---------------------------------------|
| 3GPP    | 3rd Generation Partnership Project    |
| AES     | Advanced Encryption Standard          |
| CA      | Certificate Authority                 |
| CRL     | Certificate Revocation List           |
| DAG     | Directed Acyclic Graph                |
| DLT     | Distributed Ledger Technology         |
| DID     | Decentralized Identifier              |
| DTLS    | Datagram Transport Layer Security     |
| IoT     | Internet of Things                    |
| IoV     | Internet of Vehicles                  |
| ISL     | Inter Satellite Link                  |
| JWT     | JSON Web Tokens                       |
| LDAP    | Lightweight Directory Access Protocol |
| LEO     | Low Earth Orbit                       |

|        |                             |
|--------|-----------------------------|
| LPWAN  | Low-Power Wide-Area Network |
| M2M    | Machine to Machine          |
| MAC    | Message Authentication Code |
| NAC    | Network Access Control      |
| NB IoT | Narrowband IoT              |
| NTN    | Non Terrestrial Networks    |
| PKI    | Public Key Infrastructure   |
| SSI    | Self Sovereign Identity     |
| TLS    | Transport Layer Security    |
| VC     | Verifiable Credential       |
| VP     | Verifiable Presentation     |
| ZTA    | Zero Trust Architecture     |

## References

1. Qu Z, Zhang G, Cao H, Xie J. LEO satellite constellation for internet of things. *IEEE Access*. 2017;5:18391–401. doi:10.1109/ACCESS.2017.2735988.
2. Khan F, Hervella C, Diez L, Fernández F, Marciano NJH, Jacobsen RH, et al. Realistic assessment of transport protocols performance over LEO-based communications. *Comput Netw*. 2023;236(7):110008. doi:10.1016/j.comnet.2023.110008.
3. Lacuna Space. Lacuna space: IoT satellite connectivity. [cited 2025 Mar 1]. Available from: <https://lacuna-space.com/>.
4. Cui J, Yu J, Zhong H, Wei L, Liu L. Chaotic map-based authentication scheme using physical unclonable function for internet of autonomous vehicle. *IEEE Trans Intell Transp Syst*. 2023;24(3):3167–81. doi:10.1109/TITS.2022.3227949.
5. Ahmed ST, Ahmed AA, Annamalai A, Chouikha M. Efficient rebroadcast location-unaware protocol for LoRaWAN mesh networks in the IoT domain. In: 2024 IEEE 14th Symposium on Computer Applications & Industrial Electronics (ISCAIE); 2024 May 24–25; Penang, Malaysia. p. 104–10. doi:10.1109/ISCAIE61308.2024.10576269.
6. Pablo Becoña J, Grané M, Miguez M, Arnaud A. Sigfox, and NB-IoT: an empirical comparison for IoT LPWAN technologies in the agribusiness. *IEEE Embedd Syst Lett*. 2024;16(3):283–6. doi:10.1109/LES.2024.3394446.
7. Li CF, Hwang JK. Implementation and verification of an SDR-based NB-IoT gNB with two-stage band-edge filter for GEO-relayed NTN scenario. In: 2024 IEEE International Conference on Microwaves, Communications, Antennas, Biomedical Engineering and Electronic Systems (COMCAS); 2024 Jul 9–11; Tel Aviv, Israel. p. 1–6. doi:10.1109/COMCAS58210.2024.10666233.
8. Li CF, Hwang JK, Ma C. NB-IoT NTN band-edge attenuation/EVM tradeoff with real-system verification. In: 2023 25th International Conference on Advanced Communication Technology (ICACT); 2023 Feb 19–22; Pyeongchang, Republic of Korea. p. 74–8. doi:10.23919/ICACT56868.2023.10079567.
9. Guo J, Chang L, Song Y, Yao S, Zheng Z, Hao Y, et al. AHA-BV: access and handover authentication protocol with batch verification for satellite-terrestrial integrated networks. *Comput Stand Interfaces*. 2025;91(9):103870. doi:10.1016/j.csi.2024.103870.
10. Ragothaman K, Wang Y, Rimal B, Lawrence M. Access control for IoT: a survey of existing research, dynamic policies and future directions. *Sensors*. 2023;23(4):1805. doi:10.3390/s23041805.
11. Ouyang M, Zhang R, Wang B, Liu J, Huang T, Liu L, et al. Network coding-based multipath transmission for LEO satellite networks with domain cluster. *IEEE Internet Things J*. 2024;11(12):21659–73. doi:10.1109/JIOT.2024.3378177.
12. Kumar R, Arnon S. Authentication method for spoofing protection in communication and navigation satellites: utilizing atmospheric signature. *Eng IEEE Commun Lett*. 2024;28(1):128–32. doi:10.1109/LCOMM.2023.3334870.

13. Suhaimi NHS, Kamarudin NH, Khalid MNA, Tahir I, Mohamed MAA. State-of-the-art authentication measures in satellite communication networks: a comprehensive analysis. *IEEE Access*. 2024;12:142241–64. doi:10.1109/ACCESS.2024.3467253.
14. Guo W, Xu J, Pei Y, Yin L, Jiang C, Ge N. A distributed collaborative entrance defense framework against DDoS attacks on satellite internet. *IEEE Internet Things J*. 2022;9(17):15497–510. doi:10.1109/JIOT.2022.3176121.
15. Ding X, Ren Y, Xie X, Zou Y, Jia M, Zhang G. Improving user capacity of satellite internet of things via joint user grouping and multi-beam processing. *IEEE Trans Commun*. 2024;72(7):3957–69. doi:10.1109/TCOMM.2024.3370445.
16. Ahmad I, Suomalainen J, Porambage P, Gurtov A, Huusko J, Höyhty M. Security of satellite-terrestrial communications: challenges and potential solutions. *IEEE Access*. 2022;10(4):96038–52. doi:10.1109/ACCESS.2022.3205426.
17. Adeniyi JK, Ajagbe SA, Adeniyi EA, Mudali P, Adigun MO, Adeniyi TT, et al. A biometrics-generated private/public key cryptography for a blockchain-based e-voting system. *Egypt Inform J*. 2024;25(24):100447. doi:10.1016/j.eij.2024.100447.
18. Garah A, Mbarek N, Kirgizov S. Enhancing IoT data confidentiality and energy efficiency through decision tree-based self-management. *Internet Things*. 2024;26(4):101219. doi:10.1016/j.iot.2024.101219.
19. Abdallah W. A physical layer security scheme for 6G wireless networks using post-quantum cryptography. *Comput Commun*. 2024;218(5):176–87. doi:10.1016/j.comcom.2024.02.019.
20. Jiang C, Zhang C, Mu L, Zhang Z, Ge J. Aerial RIS-aided physical layer security design for satellite communication among similar channels. *J Inf Intell*. 2023;1(1):54–67. doi:10.1016/j.jiixd.2022.11.001.
21. Driouch O, Bah S, Guennoun Z. CANSat-IDS: an adaptive distributed intrusion detection system for satellites, based on combined classification of CAN traffic. *Comput Secur*. 2024;146(4):104033. doi:10.1016/j.cose.2024.104033.
22. Garcia-del-Real J, Alcaráz M. Unlocking the future of space resource management through satellite remote sensing and AI integration. *Resour Policy*. 2024;91(1):104947. doi:10.1016/j.resourpol.2024.104947.
23. Liu Y, Ni L, Peng M. A secure and efficient authentication protocol for satellite-terrestrial networks. *IEEE Internet Things J*. 2023;10(7):5810–22. doi:10.1109/JIOT.2022.3152900.
24. Kalmykov IA, Olenov AA, Kononova NV, Peleshenko TA, Dukhovnyj DV, Chistousov NK, et al. Improvement of the cybersecurity of the satellite internet of vehicles through the application of an authentication protocol based on a modular error-correction code. *World Electr Veh J*. 2024;15(7):278. doi:10.3390/wevj15070278.
25. Xiong T, Zhang R, Liu J, Huang T, Liu Y, Yu FR. A blockchain-based and privacy-preserved authentication scheme for inter-constellation collaboration in space-ground integrated networks. *Comput Netw*. 2022;206(2):108793. doi:10.1016/j.comnet.2022.108793.
26. Carlo A, Obergfaell K. Cyber attacks on critical infrastructures and satellite communications. *Int J Crit Infrastruct Prot*. 2024;46(22):100701. doi:10.1016/j.ijcip.2024.100701.
27. Bernabé Murcia JM, Cánovas E, García-Rodríguez J, M.Zarca A, Skarmeta A. Decentralised identity management solution for zero-trust multi-domain computing continuum frameworks. *Future Gener Comput Syst*. 2025;162(2):107479. doi:10.1016/j.future.2024.08.003.
28. Sealey N, Aijaz A, Holden B. IOTA Tangle 2.0: toward a scalable, decentralized, smart, and autonomous IoT ecosystem. In: 2022 International Conference on Smart Applications, Communications and Networking (SmartNets); 2022 Nov 29–Dec 1; Palapye, Botswana. p. 1–8. doi:10.1109/SmartNets55823.2022.9994016.
29. Raschendorfer A, Mörzinger B, Steinberger E, Pelzmann P, Oswald R, Stadler M, et al. On IOTA as a potential enabler for an M2M economy in manufacturing. In: *Procedia CIRP* 2019; 79. 12th CIRP Conference on Intelligent Computation in Manufacturing Engineering; 2018 Jul 18–20; Gulf of Naples, Italy. p. 379–84. doi:10.1016/j.procir.2019.02.096.
30. Hoang AT, Ileri CU, Sanders W, Schulte S. zkSSI: a zero-knowledge-based self-sovereign identity framework. In: 2024 IEEE International Conference on Blockchain (Blockchain); 2024 Aug 19–22; Copenhagen, Denmark. p. 276–85. doi:10.1109/Blockchain62396.2024.00043.

31. Yu Y, Zhao Y, Li Y, Du X, Wang L, Guizani M. Blockchain-based anonymous authentication with selective revocation for smart industrial applications. *IEEE Trans Ind Inform.* 2020;16(5):3290–300. doi:10.1109/TII.2019.2944678.
32. Bian Y, Wang X, Jin JX, Jiao Z, Duan S. Flexible and scalable decentralized identity management for industrial internet of things. *IEEE Internet Things J.* 2024 Aug;11(16):27058–72. doi:10.1109/jiot.2024.3399535.
33. Sarfraz U, Alam M, Zeadally S, Khan A. Privacy aware IOTA ledger: decentralized mixing and unlinkable IOTA transactions. *Comput Netw.* 2019;148:361–72. doi:10.1016/j.comnet.2018.11.019.
34. Friha O, Ferrag MA, Shu L, Maglaras L, Wang X. Internet of things for the future of smart agriculture: a comprehensive survey of emerging technologies. *IEEE/CAA J Autom Sin.* 2021;8(4):718–52. doi:10.1109/JAS.2021.1003925.
35. Susilo HE, Suryana J. Research on LPWAN direct to satellite IoT: a survey technology and performance on LEO satellite. In: 2023 29th International Conference on Telecommunications (ICT); 2023 Nov 8–9; Toba, Indonesia. p. 1–7. doi:10.1109/ICT60153.2023.10374072.
36. Elijah O, Rahim SKA, Musa MJ, Salihu YO, Bello MJ, Sani MY. Development of LoRa-sigfox IoT device for long distance applications. In: 2022 IEEE Nigeria 4th International Conference on Disruptive Technologies for Sustainable Development (NIGERCON); 2022 Apr 5–7; Abuja, Nigeria. p. 1–5. doi:10.1109/NIGERCON54645.2022.9803173.
37. Centenaro M, Costa CE, Granelli F, Sacchi C, Vangelista L. A survey on technologies, standards and open challenges in satellite IoT. *IEEE Commun Surv Tutor.* 2021;23(3):1693–720. doi:10.1109/COMST.2021.3078433.
38. Jagatheesaperumal SK, Pham QV, Ruby R, Yang Z, Xu C, Zhang Z. Explainable AI over the internet of things (IoT): overview, state-of-the-art and future directions. *IEEE Open J Commun Soc.* 2022;3:2106–36. doi:10.1109/OJCOMS.2022.3215676.
39. Lee J, Noh S, Jung S, Lee N. Coverage analysis of LEO satellite downlink networks: orbital geometry dependent approach. *IEEE Access.* 2024;12:196939–53. doi:10.1109/ACCESS.2024.3522377.
40. Fraire JA, Iova O, Valois F. Space-terrestrial integrated internet of things: challenges and opportunities. *IEEE Commun Mag.* 2022;60(12):64–70. doi:10.1109/MCOM.008.2200215.
41. Asad Ullah M, Pasolini G, Mikhaylov K, Alves H. Understanding the limits of LoRA direct-to-satellite: the doppler Perspectives. *IEEE Open J Commun Soc.* 2024;5:51–63. doi:10.1109/OJCOMS.2023.3337004.
42. Deng R, Di B, Zhang H, Kuang L, Song L. Ultra-dense LEO satellite constellations: how many LEO satellites do we need? *IEEE Trans Wirel Commun.* 2021;20(8):4843–57. doi:10.1109/TWC.2021.3062658.
43. García-Teodoro P, Camacho J, Maciá-Fernández G, Gómez-Hernández J, López-Marín V. A novel zero-trust network access control scheme based on the security profile of devices and users. *Comput Netw.* 2022;212(1):109068. doi:10.1016/j.comnet.2022.109068.
44. Maldonado-Ruiz D, Torres J, El Madhoun N, Badra M. Current trends in blockchain implementations on the paradigm of public key infrastructure: a survey. *IEEE Access.* 2022;10:17641–55. doi:10.1109/ACCESS.2022.3145156.
45. IEEE standard for local and Metropolitan area networks—port-based network access control. [Internet]. [cited 2025 Jun 15]. Available from: <https://standards.ieee.org/ieee/802.1X/7345/>.
46. Mazzocca C, Acar A, Uluagac S, Montanari R, Bellavista P, Conti M. A survey on decentralized identifiers and verifiable credentials. *IEEE Commun Surv Tutor.* 2025;1. doi:10.1109/COMST.2025.3543197.
47. Bandara E, Liang X, Foytik P, Shetty S, Zoysa KD. A blockchain and self-sovereign identity empowered digital identity platform. In: 2021 International Conference on Computer Communications and Networks (ICCCN); 2021 Jul 19–22; Online. p. 1–7. doi:10.1109/ICCCN52240.2021.9522184.
48. Ramírez-Gordillo T, Maciá-Lillo A, Pujol FA, García-D’Urso N, Azorín-López J, Mora H. Decentralized identity management for internet of things (IoT) devices using IOTA blockchain technology. *Future Internet.* 2025;17(1):49. doi:10.3390/fi17010049.
49. Kovačević A, Gligorić N, Jokić S. Decentralized identities for enhanced security in vehicle-to-everything (V2X). In: 2024 32nd Telecommunications Forum (TELFOR); 2024 Nov 26–27; Belgrade, Serbia. p. 1–4. doi:10.1109/TELFOR63250.2024.10819049.

50. Alani DS, Sagheer AM. Public key infrastructure approaches based on blockchain. In: 21st International Multi-Conference on Systems, Signals & Devices (SSD); 2024 Apr 22–25; Erbil, Iraq. p. 369–75. doi:10.1109/SSD61670.2024.10549485.
51. Herbke P, Cory T, Migliardi M. Decentralized credential status management: a paradigm shift in digital trust. In: 6th Conference on Blockchain Research & Applications for Innovative Networks and Services (BRAINS); 2024 Oct 9–11; Berlin/Heidelberg, Germany. p. 1–10. doi:10.1109/BRAINS63024.2024.10732832.
52. Astorga J, Barcelo M, Urbieta A, Jacob E. Revisiting the feasibility of public key cryptography in light of IIoT communications. *Sensors*. 2022;22(7):2561. doi:10.3390/s22072561.
53. Kim GH. A comprehensive survey of cryptography key management in decentralized identity ecosystem. In: Fujita H, Watanobe Y, Ali M, Wang Y, editors. *Advances and trends in artificial intelligence. theory and applications*. Singapore: Springer Nature Singapore; 2025. p. 128–40. doi:10.1007/978-981-96-8892-0\_11.
54. Cuñat S, Reinosa R, Lacalle I, Palau CE. Immutability and non-repudiation in the exchange of key messages within the EU IoT-edge-cloud continuum. In: *Proceedings of the 19th International Conference on Availability, Reliability and Security*; 2024 Jul 30–Aug 2; Vienna, Austria. Vienna, Austria: Association for Computing Machinery; 2024. doi:10.1145/3664476.3669918.
55. Yildiz H, Küpper A, Thatmann D, Göndör S, Herbke P. Toward interoperable self-sovereign identities. *IEEE Access*. 2023;11:114080–116. doi:10.1109/ACCESS.2023.3313723.
56. Gligoric N, Escuín D, Polo L, Amditis A, Georgakopoulos T, Fraile A. IOTA-based distributed ledger in the mining industry: efficiency, sustainability and transparency. *Sensors*. 2024;24(3):923. doi:10.3390/s24030923.
57. Kailus A, Kern D, Krauß C. Self-sovereign identity for electric vehicle charging. In: Pöpper C, Batina L, editors. *Applied cryptography and network security*. Cham, Switzerland: Springer Nature; 2024. p. 137–62. doi:10.1007/978-3-031-54776-8\_6.
58. Ansar K, Ahmed M, Malik SUR, Helfert M, Kim J. Blockchain based general data protection regulation compliant data breach detection system. *PeerJ Comput Sci*. 2024;10:e1882. doi:10.7717/peerj-cs.1882.
59. Asaju BJ. Addressing public key infrastructure (PKI) challenges in V2X networks: strategies for scalability, certificate management, and trusted authorities. *J Sci Technol*. 2024;5:69–86.
60. Ding Y, Zhang Y, Qin B, Wang Q, Yang Z, Shi W. A scalable cross-chain access control and identity authentication scheme. *Sensors*. 2023;23(4):2000. doi:10.3390/s23042000.
61. Kovach A, Lanza J, Montalvillo L, Urbieta A. Sovereign IIoT data exchange using DAG-based DLT and international data spaces architecture. In: *Proceedings of the 4th Eclipse Security, AI, Architecture and Modelling Conference on Data Space*; 2024 Oct 22; Mainz, Germany. Mainz, Germany: Association for Computing Machinery; 2024. p. 76–85. doi:10.1145/3685651.3686658.
62. Dhote S, Maidamwar P, Thakur S. An empirical review of security models used for issuing tamper proof certificates for authentic credentials. In: *2024 2nd International Conference on Intelligent Data Communication Technologies and Internet of Things (IDCIoT)*; 2024 Jan 4–6; Bengaluru, India. p. 486–92. doi:10.1109/IDCIoT59759.2024.10467298.
63. Kang M, Park S, Lee Y. A survey on satellite communication system security. *Sensors*. 2024;24(9):2897. doi:10.3390/s24092897.
64. Höglund J, Bouget S, Furuheid M, Preuß Mattsson J, Selander G, Raza S. AutoPKI: public key infrastructure for IoT with automated trust transfer. *Int J Inf Secur*. 2024;23(3):1859–75. doi:10.1007/s10207-024-00825-z.
65. Venkatraman S, Parvin S. Developing an IoT identity management system using blockchain. *Systems*. 2022;10(2):39. doi:10.3390/systems10020039.
66. Sabrina F, Li N, Sohail S. A blockchain based secure IoT system using device identity management. *Sensors*. 2022;22(19):7535. doi:10.3390/s22197535.
67. Song H, Tu Z, Qin Y. Blockchain-based access control and behavior regulation system for IoT. *Sensors*. 2022;22(21):8339. doi:10.3390/s22218339.
68. Khan A, Tahir S, Khan F, Tahir H, Zulkifl Z. Enhancing security of cloud-based IoT systems through network access control (NAC). In: *2021 International Conference on Communication Technologies (ComTech)*; 2021 Sep 21–22; Rawalpindi, Pakistan. p. 103–8. doi:10.1109/ComTech52583.2021.9616855.

69. Huang T, Xie R, Ren Y, Yu FR, Zou Z, Han L, et al. DTAIS: distributed trusted active identity resolution systems for the industrial internet. *Digit Commun Netw*. 2024;10(4):853–62. doi:10.1016/j.dcan.2023.06.006.
70. Bhutta MNM, Khwaja AA, Nadeem A, Ahmad HF, Khan MK, Hanif MA, et al. A survey on blockchain technology: evolution, architecture and security. *IEEE Access*. 2021;9:61048–73. doi:10.1109/ACCESS.2021.3072849.
71. World Wide Web Consortium (W3C). Web standards. [cited 2025 May 6]. Available from: <https://www.w3.org/standards/>.
72. Kersic V, Vidovic U, Vrecko A, Domajnko M, Turkanovic M. Orchestrating digitalwallets for on- and off-chain decentralized identity management. *IEEE Access*. 2023;11:78135–51. doi:10.1109/ACCESS.2023.3299047.
73. Alizadeh M, Andersson K, Schelén O. Comparative analysis of decentralized identity approaches. *IEEE Access*. 2022;10(3):92273–83. doi:10.1109/ACCESS.2022.3202553.
74. Berbecaru DG, Lioy A. An evaluation of X.509 certificate revocation and related privacy issues in the web PKI ecosystem. *IEEE Access*. 2023;11:79156–75. doi:10.1109/ACCESS.2023.3299357.
75. Naik N, Jenkins P. uPort open-source identity management system: an assessment of self-sovereign identity and user-centric data platform built on blockchain. In: 2020 IEEE International Symposium on Systems Engineering (ISSE); 2020 Oct 12–Nov 12; Online. p. 1–7. doi:10.1109/ISSE49799.2020.9272223.
76. Ceramic Network. How it works. [cited 2025 Aug 18]. Available from: <https://ceramic.network/how-it-works>.
77. Franklin SSP, Shamala LM, Sree TR. Decentralized certificate issuance and verification system using Ethereum blockchain technology. *J Netw Comput Appl*. 2025;242(1):104190. doi:10.1016/j.jnca.2025.104190.
78. Wylde A. Zero trust: never trust, always verify. In: International Conference on Cyber Situational Awareness, Data Analytics and Assessment (CyberSA); 2021 Jun 14–18; Dublin, Ireland. p. 1–4. doi:10.1109/CyberSA52016.2021.9478244.
79. Alevizos L, Eiza MH, Ta VT, Shi Q, Read J. Blockchain-enabled intrusion detection and prevention system of APTs within zero trust architecture. *IEEE Access*. 2022;10(2):89270–88. doi:10.1109/ACCESS.2022.3200165.
80. Aleisa MA. Blockchain-enabled zero trust architecture for privacy-preserving cybersecurity in IoT environments. *IEEE Access*. 2025;13(4):18660–76. doi:10.1109/ACCESS.2025.3529309.
81. Syed NF, Shah SW, Shaghaghi A, Anwar A, Baig Z, Doss R. Zero trust architecture (ZTA): a comprehensive survey. *IEEE Access*. 2022;10(3):57143–79. doi:10.1109/ACCESS.2022.3174679.
82. Abboud S, Abdoun N. Enhancing LoRaWAN security: an advanced AES-based cryptographic approach. *IEEE Access*. 2024;12(1):2589–606. doi:10.1109/ACCESS.2023.3348416.
83. Ren X, Cao J, Ma M, Li H, Zhang Y. A novel PUF-based group authentication and data transmission scheme for NB-IoT in 3GPP 5G networks. *IEEE Internet Things J*. 2022;9(5):3642–56. doi:10.1109/JIOT.2021.3098224.
84. Rochman S, Istiyanto JE, Dharmawan A, Handika V, Purnama SR. Optimization of tips selection on the IOTA tangle for securing blockchain-based IoT transactions. *Procedia Comput Sci*. 2023;216:230–6. doi:10.1016/j.procs.2022.12.131.
85. Helmer L, Penzkofer A. Report on the energy consumption of the IOTA 2.0 prototype network (GoShimmer 0.8.3) under different testing scenarios. arXiv:2210.13996. 2022.
86. Alshaikhli M, Elfouly T, Elharrouss O, Mohamed A, Ottakath N. Evolution of internet of things from blockchain to IOTA: a survey. *IEEE Access*. 2022;10(2):844–66. doi:10.1109/ACCESS.2021.3138353.
87. Chen Y, Wang Y, Sun B, Liu J. Addressing the transaction validation issue in IOTA tangle: a tip selection algorithm based on time division. *Mathematics*. 2023;11(19):4116. doi:10.3390/math11194116.
88. Claudio A, Vesco A. A novel DID method leveraging the IOTA tangle and its integration into OpenSSL. In: Machado JM, Prieto J, Vieira P, Peixoto H, Abelha A, Arroyo D, editors. Blockchain and applications, 5th international congress. Cham, Switzerland: Springer Nature; 2023. p. 394–404. doi:10.1007/978-3-031-45155-3\_38.
89. Tang Q, Fei Z, Li B, Han Z. Computation offloading in LEO satellite networks with hybrid cloud and edge computing. *IEEE Internet Things J*. 2021;8(11):9164–76. doi:10.1109/JIOT.2021.3056569.
90. Zhang Y, Nakanishi R, Sasabe M, Kasahara S. Combining IOTA and attribute-based encryption for access control in the Internet of things. *Sensors*. 2021;21(15):5053. doi:10.3390/s21155053.
91. Lin BY, Dziubałtowska D, Macek P, Penzkofer A, Müller S. Robustness of the tangle 2.0 consensus. tech. rep. Wrocław, Poland: Wrocław University of Science and Technology; 2022. doi:10.1007/978-3-031-31234-2\_16.

92. Kua J, Loke SW, Arora C, Fernando N, Ranaweera C. Internet of things in space: a review of opportunities and challenges from satellite-aided computing to digitally-enhanced space living. *Sensors*. 2021;21(23):8117. doi:10.3390/s21238117.
93. Hui M, Zhai S, Wang D, Hui T, Wang W, Du P, et al. A review of LEO-satellite communication payloads for integrated communication, navigation, and remote sensing: opportunities, challenges, future directions. *IEEE Internet Things J*. 2025;12(12):18954–92. doi:10.1109/JIOT.2025.3553942.
94. Zhou Z, Wang N, Liu J, Zhou W, Fu J, Deng L. Conditional privacy-preserving and efficient distributed IoV data sharing scheme based on a hierarchical and zonal blockchain. *Veh Commun*. 2024;49:100832. doi:10.1016/j.vehcom.2024.100832.
95. Sharma P, Wilfred Godfrey W, Trivedi A. When blockchain meets IoT: a comparison of the performance of communication protocols in a decentralized identity solution for IoT using blockchain. *Cluster Comput*. 2024;27:269–84. doi:10.1007/s10586-022-03921-8.
96. Alshaikhli M, Al-Maadeed S, Saleh M. Enhancing scalability and network efficiency in IOTA tangle networks: a POMDP-based tip selection algorithm. *Computers*. 2025;14(4):117. doi:10.3390/computers14040117.
97. Raikwar M, Polyanskii N, Müller S. SoK: dag-based consensus protocols. In: 2024 IEEE International Conference on Blockchain and Cryptocurrency (ICBC); 2024 May 27–31; Dublin, Ireland. p. 1–18. doi:10.1109/ICBC59979.2024.10634358.
98. Chen Q, Yang L, Liu X, Cheng B, Guo J, Li X. Modeling and analysis of inter-satellite link in LEO satellite networks. In: 13th International Conference on Communication Software and Networks (ICCSN); 2021 Jun 4–7; Chongqing, China. p. 134–8. doi:10.1109/ICCSN52437.2021.9463648.